

**CHARACTERIZATION OF THE ARSENATE REDUCTASE  
OF *E. COLI* PLASMID R773**

by

**Domenic Perri**

**A Thesis  
Submitted to the College of Graduate Studies and Research  
Through the Department of Chemistry and Biochemistry  
In Partial Fulfillment of the Requirements for the  
Degree of Master of Science at the  
University of Windsor**

**Windsor, Ontario, Canada**

**1999**



National Library  
of Canada

Acquisitions and  
Bibliographic Services

395 Wellington Street  
Ottawa ON K1A 0N4  
Canada

Bibliothèque nationale  
du Canada

Acquisitions et  
services bibliographiques

395, rue Wellington  
Ottawa ON K1A 0N4  
Canada

*Your file* *Votre référence*

*Our file* *Notre référence*

The author has granted a non-exclusive licence allowing the National Library of Canada to reproduce, loan, distribute or sell copies of this thesis in microform, paper or electronic formats.

The author retains ownership of the copyright in this thesis. Neither the thesis nor substantial extracts from it may be printed or otherwise reproduced without the author's permission.

L'auteur a accordé une licence non exclusive permettant à la Bibliothèque nationale du Canada de reproduire, prêter, distribuer ou vendre des copies de cette thèse sous la forme de microfiche/film, de reproduction sur papier ou sur format électronique.

L'auteur conserve la propriété du droit d'auteur qui protège cette thèse. Ni la thèse ni des extraits substantiels de celle-ci ne doivent être imprimés ou autrement reproduits sans son autorisation.

0-612-52631-3

Canada

© Domenic Perri 1999  
All Rights Reserved

## **ABSTRACT**

### **CHARACTERIZATION OF THE ARSENATE REDUCTASE OF *E. COLI* PLASMID R773**

**by**

**Domenic Perri**

Bacterial resistance to toxic anions in *Escherichia coli* is carried on the R773 plasmid. The plasmid contains the *ars* operon, which encodes a group of proteins responsible for the extrusion of arsenicals and antimonials out of the cell. One of these proteins, ArsC, has been shown to reduce arsenate ( $\text{AsO}_4^{3-}$ ) to arsenite ( $\text{AsO}_2^-$ ) prior to being transported out of the cell (Gladysheva *et al.*, 1994). The protein requires glutathione (GSH) and glutaredoxin in order to reduce the toxic oxyanions.

Circular dichroism experiments demonstrated that the secondary structure of ArsC changed marginally when either the substrate or product was present. The melting temperature of ArsC also remained unchanged upon the addition of either arsenate or arsenite. The reduction of arsenate to arsenite by ArsC involves glutathione, glutaredoxin-1, and arsenate. Fluorescence spectroscopy of Trp-mutated ArsC containing 7-azatryptophan was used to probe its interaction with glutaredoxin-1. The results suggest that there is a direct interaction between glutathione with ArsC. There is no change in the fluorescence of the Trp-mutants of ArsC upon the addition of glutaredoxin-1, suggesting that there is no direct interaction of glutaredoxin-1 with ArsC.

## **Dedication**

**To my parents, whose love and support  
will always be appreciated.**

## **ACKNOWLEDGEMENTS**

I would like to express my sincerest gratitude to Dr. Lana Lee who displayed great patience and guidance throughout the course of this study. It has been an honour and a privilege to be a graduate student in her lab.

I would also like to acknowledge the other members of my committee, Dr. Bulent Mutus and Dr. Alden Warner for taking the time to read and evaluate this thesis.

I am very grateful to Pawel Malinowski, Mauro Acchione, and Dr. Arthur Szabo, whose keen insight into molecular biology and fluorescence spectroscopy was tremendously helpful. Their friendship is also greatly appreciated.

I would also like to thank the friends that I have made along the way: Christopher Deslippe, Michael Siwek, Dave "Beebs" Michels, Natalie Labbe, Marie Tannous, Zayna Khayat, Jeff Baldwin, Mike Weller, Bahe Rajendran, Sherri Udell, and Nicole Doyon (I apologize if I've forgotten anyone). Your friendship and patience is appreciated.

Thanks also to my dear friends Peter and Darlene Schiavo, whose friendship and support over the years have not gone unnoticed. Thank you for being such wonderful friends. Finally, I thank my siblings Joanne, Marco, and Tony whom I love dearly and whose patience and friendship I will always cherish.

## TABLE OF CONTENTS

		<b>Page</b>
ABSTRACT		iv
DEDICATION		v
ACKNOWLEDGEMENTS		vi
LIST OF TABLES		xi
LIST OF FIGURES		xii
LIST OF ABBREVIATIONS		xiv
 CHAPTER		
1	<b>Introduction</b>	1
2	<b>Materials and Methods</b>	9
	<b>Materials</b>	9
	<b>Methods</b>	11
	<b>Polyacrylamide Electrophoresis</b>	11
	<b>Agarose Electrophoresis</b>	13
	<b>Isolation of <i>E. coli</i> ArsC and <i>E. coli</i> Grx-1</b>	14
	<b>Overexpression and Purification of Wild Type <i>E. coli</i> ArsC</b>	14
	<b>Overexpression and Purification of <i>E. coli</i> Grx-1</b>	15
	<b>Protein Assay</b>	16
	<b>Plasmid Isolation</b>	16
	<b>Site-Directed Mutagenesis of <i>E. coli</i> ArsC</b>	17

	<b>Primer Selection for A11W ArsC Mutant</b>	<b>18</b>
	<b>Primer Selection for Y7W ArsC Mutant</b>	<b>20</b>
	<b>Basic Protocol for Site-Directed Mutagenesis</b>	<b>20</b>
	<b>Bacterial Transformation</b>	<b>24</b>
	<b>Procedure for Preparing Competent Cells</b>	<b>25</b>
	<b>Procedure for Transformation of Trp Auxotroph With p<i>ArsC</i> Plasmid</b>	<b>25</b>
	<b>Preparation of Glycerol Stocks</b>	<b>26</b>
	<b>Incorporation of Trp Analogs Using M9 Medium</b>	<b>26</b>
	<b>Amino Acid Analysis of <i>E. coli</i> ArsC</b>	<b>27</b>
	<b>Secondary Structure Prediction of <i>E. coli</i> ArsC</b>	<b>30</b>
	<b>CD Spectroscopy</b>	<b>31</b>
	<b>Thermal Denaturations of <i>E. coli</i> ArsC</b>	<b>32</b>
	<b>Fluorescence Studies of ArsC</b>	<b>33</b>
<b>3</b>	<b>Results</b>	<b>34</b>
	<b>Overexpression and Purification of Wild Type <i>E. coli</i> ArsC</b>	<b>34</b>
	<b>SDS-PAGE of Wild Type <i>E. coli</i> ArsC</b>	<b>34</b>
	<b>Overexpression and Purification of <i>E. coli</i> Grx-1</b>	<b>38</b>
	<b>SDS-PAGE of <i>E. coli</i> Grx-1</b>	<b>38</b>
	<b>Amino Acid Analysis of <i>E. coli</i> ArsC</b>	<b>42</b>
	<b>Secondary Structure Predictions Using Algorithms</b>	<b>45</b>
	<b>Circular Dichroism Studies of <i>E. coli</i> ArsC</b>	<b>50</b>



	<b>Thermal Denaturations of <i>E. coli</i> ArsC</b>	<b>53</b>
	<b>Isolation of Plasmid R773</b>	<b>55</b>
	<b>Transformation of Trp Auxotroph with A11W and Y7W Mutated <i>E. coli</i> ArsC</b>	<b>60</b>
	<b>Isolation of ArsC A11W and Y7W Mutants</b>	<b>60</b>
	<b>Fluorescence Studies of <i>E. coli</i> ArsC Mutants With <i>E. coli</i> Grx-1</b>	<b>60</b>
	<b>Fluorescence Emission Spectra of Mutant and Wild-Type <i>E. coli</i> ArsC</b>	<b>60</b>
	<b>Fluorescence Studies of 7AW-A11W ArsC With <i>E. coli</i> Grx-1</b>	<b>63</b>
	<b>Fluorescence Studies of 7AW-Y7W ArsC With <i>E. coli</i> Grx-1</b>	<b>65</b>
	<b>Glutathione Titrations of <i>E. coli</i> ArsC Mutants</b>	<b>68</b>
<b>4</b>	<b>Discussion</b>	<b>70</b>
	<b>Overexpression and Purification of Proteins</b>	<b>70</b>
	<b>SDS-PAGE of Protein Samples</b>	<b>71</b>
	<b>Amino Acid Analysis of <i>E. coli</i> ArsC</b>	<b>72</b>
	<b>Secondary Structural Studies of <i>E. coli</i> ArsC</b>	<b>73</b>
	<b>Prediction of Secondary Structures</b>	<b>73</b>
	<b>Circular Dichroism Studies of <i>E. coli</i> ArsC</b>	<b>75</b>
	<b>Thermal Denaturations of <i>E. coli</i> ArsC</b>	<b>77</b>
	<b>Isolation and Site-Directed Mutagenesis of R773 Plasmid Containing the <i>ArsC</i> Gene</b>	<b>77</b>
	<b>Transformation of Trp Auxotroph with A11W and Y7W Mutants of ArsC</b>	<b>78</b>
	<b>Isolation of A11W and Y7W Mutants</b>	<b>78</b>

	<b>Fluorescence Studies of Trp-containing <i>E. coli</i> ArsC</b>	<b>78</b>
	<b>Glutathione Titrations of <i>E. coli</i> ArsC</b>	<b>79</b>
	<b>Conclusions</b>	<b>80</b>
	<b>Future Work</b>	<b>81</b>
<b>REFERENCES</b>		<b>84</b>
<b>VITA AUCTORIS</b>		<b>92</b>

## LIST OF TABLES

<b>TABLE</b>	<b>TITLE</b>	<b>PAGE</b>
2-1	<b>PCR Cycling Parameters for Quik-Change Mutagenesis Kit</b>	23
2-2	<b>Elution Conditions Used for Amino Acid Analysis Using the Pico-Tag™ System and 441 Detector</b>	29
3-1	<b>Amino Acid Analysis of <i>E. coli</i> ArsC</b>	44
3-2a	<b>Residue Assignments of the Secondary Structure Prediction of <i>E. coli</i> ArsC by various Algorithms</b>	48
3-2b	<b>Secondary Structure Prediction of <i>E. coli</i> ArsC by various Algorithms</b>	49
3-3	<b>Experimentally Determined Secondary Structure of <i>E. coli</i> ArsC</b>	51
3-4	<b>Experimentally Determined Melting Temperatures of <i>E. coli</i> ArsC</b>	56

## LIST OF FIGURES

FIGURE	TITLE	PAGE
1-1	Primary Structure of <i>E. coli</i> ArsC	3
1-2	Tryptophan and Tryptophan Analogs	6
2-1	Alignment of the primary sequence of <i>E. coli</i> ArsC with the <i>ArsC</i> gene displaying the A11W primer selection	19
2-2	Alignment of the primary sequence of <i>E. coli</i> ArsC with the <i>ArsC</i> gene displaying the Y7WW primer selection	21
3-1	Q-Sepharose Ion Exchange Elution Profile of <i>E. coli</i> ArsC	35
3-2	Sephadex G-50 Superfine Elution Profile of <i>E. coli</i> ArsC	36
3-3	15% SDS-PAGE of <i>E. coli</i> ArsC	37
3-4	Q-Sepharose Ion Exchange Elution Profile of <i>E. coli</i> Grx-1	39
3-5	Sephadex G-50 Superfine Elution Profile of <i>E. coli</i> Grx-1	40
3-6	15% SDS-PAGE of <i>E. coli</i> Grx-1	41
3-7	Amino Acid Analysis of <i>E. coli</i> ArsC	43
3-8	Melting Curves of <i>E. coli</i> ArsC	54
3-9	Van Hoff't Plots of the Temperature Melts of <i>E. coli</i> ArsC	57
3-10	CD Spectra of <i>E. coli</i> ArsC at Various Temperatures	58
3-11	1.0% Agarose Gel of Purified R773 Plasmid containing the <i>E. coli</i> <i>ArsC</i> gene	59
3-12	15% SDS-PAGE of the A11W and Y7W mutants of <i>E. coli</i> ArsC	61
3-13	Emission Spectra of Wild Type and Trp Mutants of <i>E. coli</i> ArsC	62
3-14	Emission Spectra of the A11W <i>E. coli</i> ArsC Mutant with Various Ligands	64

3-15	<b>Emission Spectra of the A117W <i>E. coli</i> ArsC Mutant with GSH</b>	<b>66</b>
3-16	<b>Emission Spectra of the Y7W <i>E. coli</i> ArsC Mutant with Various Ligands</b>	<b>67</b>
3-17	<b>Emission Spectra of the Y7W <i>E. coli</i> ArsC mutant with different GSH concentrations</b>	<b>69</b>
4-1	<b>Proposed Mechanism of Arsenate Reduction</b>	<b>82</b>

## **LIST OF ABBREVIATIONS**

<b>4FW</b>	<b>4-fluorotryptophan</b>
<b>5OHW</b>	<b>5-hydroxytryptophan</b>
<b>6FW</b>	<b>6-fluorotryptophan</b>
<b>7AW</b>	<b>7-azatryptophan</b>
<b>ACN</b>	<b>acetonitrile</b>
<b>APS</b>	<b>ammonium persulfate</b>
<b>ArsC</b>	<b>arsenate reductase</b>
<b>bp</b>	<b>base pairs</b>
<b>CD</b>	<b>circular dichroism</b>
<b>Da</b>	<b>Daltons</b>
<b>dd-H<sub>2</sub>O</b>	<b>double-distilled water</b>
<b>DNA</b>	<b>deoxyribonucleic acid</b>
<b>DTT</b>	<b>dithiothreitol</b>
<b>EDTA</b>	<b>ethylenediaminetetraacetic Acid</b>
<b>Grx</b>	<b>glutaredoxin</b>
<b>GSH</b>	<b>glutathione</b>
<b>HCl</b>	<b>hydrochloric acid</b>
<b>HPLC</b>	<b>high-performance liquid chromatography</b>
<b>K</b>	<b>Kelvin</b>
<b>MOPS</b>	<b>(3-[N-morpholino]propanesulfonic acid</b>
<b>MRE</b>	<b>mean residue ellipticity</b>

<b>MWCO</b>	<b>molecular weight cut-off</b>
<b>PCR</b>	<b>polymerase chain reaction</b>
<b>PITC</b>	<b>phenylisothiocyanate</b>
<b>PMSF</b>	<b>phenylmethylsulfonylfluoride</b>
<b>Q-Sepharose</b>	<b>quaternary ammonium-sepharose</b>
<b>RNA</b>	<b>ribonucleic acid</b>
<b>rpm</b>	<b>revolutions per minute</b>
<b>SDS-PAGE</b>	<b>sodium dodecyl sulfate polyacrylamide gel electrophoresis</b>
<b>TBE</b>	<b>tris-borate-edta</b>
<b>TEA</b>	<b>triethylamine</b>
<b>TEMED</b>	<b>N,N,N',N'-tetramethylethylenediamine</b>
<b>Tris</b>	<b>(tris[hydroxymethyl]aminomethane)</b>
<b>Trp</b>	<b>tryptophan</b>
<b>UV</b>	<b>ultraviolet</b>

## **1.1 Introduction**

Many bacteria contain plasmids that provide the bacterium with diverse genetic benefits. These benefits include antibiotic resistance, synthesis of bacteriocins, and resistance to toxic heavy metals (Silver, 1992). Arsenic is one such metal that exerts toxic effects on cells. Arsenate is an analog of phosphate that causes the spontaneous hydrolysis of sugars once they are arsenylated (Willsky and Malamy, 1981). Arsenite is even more toxic in that it reacts readily with sulfhydryls of proteins, thereby inactivating enzymes (Knowles and Benson, 1983).

Bacterial resistance to arsenicals and similar oxyanions has been demonstrated to be carried on the R773 plasmid of *Escherichia coli* (Hedges and Baumberg, 1973) and the pI258 plasmid in *Staphylococcus aureus* (Novick and Roth, 1968). The R773 plasmid contains a 91 kbp cluster of genes that encodes an ATP-driven oxyanion pump (Mobley and Rosen, 1982). This *ars* operon encodes a chain of proteins that result in an active expulsion of toxic oxyanions from the cytoplasm of the resistant bacterium (Ji and Silver, 1992). The first of these proteins, ArsR, is a *trans*-acting repressor of the operon (Wu and Rosen, 1991). This 13 kDa protein forms a homodimer that binds to a region within the *ars* promoter, thereby repressing the transcription of the *ars* operon. Recent studies (Xu and Rosen, 1997) indicate that only the dimer of ArsR is capable of metal recognition and repression. The second protein of this operon, ArsD, is also a repressor of the *ars* operon. The 13 kDa protein differs from ArsR in that ArsR controls the basal level expression of the operon whereas ArsD controls maximal expression (Chen and Rosen, 1997). Both ArsR and ArsD bind to the same promoter region, with ArsR having



a higher affinity for the site. The two regulatory proteins regulate expression levels of the operon to within a narrow range, thus providing a sensitive mechanism for the sensing of toxic heavy metals.

ArsA, a 63 169 Da protein, has been shown to be associated with the inner membrane (Tisa and Rosen, 1990). The active form of ArsA exists as a homodimer that forms upon binding of the toxic anion (Hsu *et al.*, 1991). The 126 kDa dimer was only observed when the ArsA was incubated with antimonite or arsenite. The active dimer contains four nucleotide binding sites, two from each monomer (Li *et al.*, 1996). ArsA is the catalytic subunit that works along with ArsB to actively pump out the toxic anions (Dey *et al.*, 1994). ArsB is an integral membrane protein (San Francisco *et al.*, 1989). This protein anchors ArsA to the inner membrane and acts as the anion channel which pumps out the toxic anions (Dey *et al.*, 1994). ArsA is the ATPase that drives ArsB to pump the anions out of the cell. The active extrusion of the toxic anions is, therefore, a concerted effort between ArsA and ArsB. The expression of ArsB alone exhibited an intermediate level of arsenite resistance (Silver and Phung, 1996). This suggests that ArsB is capable of acting alone without the ATPase as a chemiosmotic transporter of the toxic heavy metal.

ArsC is required for the reduction of the toxic anions prior to their extrusion (Ji *et al.*, 1994). The ArsC protein of plasmid R773 is a 16 kDa protein (141 residues) that requires glutathione (GSH) to reduce arsenate *in vivo* (Gladeysheva *et al.*, 1994). The amino acid sequence of ArsC is shown in Figure 1-1. The fact that this protein reduces a toxic moiety into an even more toxic compound is intriguing. A reasonable assumption would be that the more toxic arsenite ( $\text{AsO}_2^-$ ) is a smaller molecule than arsenate ( $\text{AsO}_4^{3-}$ ) and, hence, more easily extruded from the cell. The protein is unique in that it does not

1  
Met-Ser-Asn-Ile-Thr-Ile-Tyr-His-Asn-Pro-Ala-Cys-Gly-Thr-Ser-Arg-  
10  
20 30  
Asn-Thr-Leu-Glu-Met-Ile-Arg-Asn-Ser-Gly-Thr-Glu-Pro-Thr-Ile-Ile-  
40  
Leu-Tyr-Leu-Glu-Asn-Pro-Pro-Ser-Arg-Asp-Glu-Leu-Val-Lys-Leu-Ile-  
50 60  
Ala-Asp-Met-Gly-Ile-Ser-Val-Arg-Ala-Leu-Leu-Arg-Lys-Asn-Val-Glu-  
70 80  
Pro-Tyr-Glu-Gln-Leu-Gly-Leu-Ala-Glu-Asp-Lys-Phe-Thr-Asp-Asp-Gln-  
90  
Leu-Ile-Asp-Phe-Met-Leu-Gln-His-Pro-Ile-Leu-Ile-Asn-Arg-Pro-Ile-  
100 110  
Val-Val-Thr-Pro-Leu-Gly-Thr-Arg-Leu-Cys-Arg-Pro-Ser-Glu-Val-Val-  
120  
Leu-Asp-Ile-Leu-Gln-Asp-Ala-Gln-Lys-Gly-Ala-Phe-Thr-Lys-Glu-Asp-  
130 140  
Gly-Glu-Lys-Val-Val-Asp-Glu-Ala-Gly-Lys-Arg-Leu-Lys

**Figure 1-1: Primary Structure of *E. coli* ArsC.** *E. coli* ArsC from the arsenical resistance plasmid R773 (Rosen *et al.*, 1991).

exhibit any significant similarities with any other known reductases and, therefore, may be a member of a new class of anion reductases.

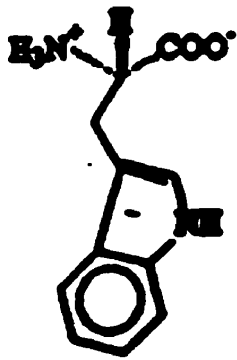
ArsC has been shown to require glutathione and only glutathione as a reducing agent to reduce oxyanions *in vivo* (Gladysheva *et al.*, 1994). *In vitro*, however, ArsC also requires the action of a protein capable of catalyzing thiol-disulfide exchange. This protein is glutaredoxin-1 (Grx-1). Glutaredoxin-1 is an 85-residue intracellular protein that functions as a glutathione-dependent hydrogen donor for several glutathione-disulfide reducing reactions (Holmgren, 1989). The Grx-1 is reduced by GSH. The oxidized GSH is, in turn, reduced by glutathione reductase with NADPH serving as the source of reducing potential. A plausible reason for the additional compounds required *in vitro* is that there are multiple glutaredoxins present in *E. coli* (Aslund *et al.*, 1994) that may serve the same function as Grx-1.

The pathway of arsenate reduction to arsenite is postulated to have at least two steps (Liu and Rosen, 1997). Arsenate is reduced to arsenite by ArsC which, in turn, becomes oxidized. The oxidized ArsC is then reduced by Grx-1, thereby regenerating the active enzyme. It has been demonstrated using fluorescence studies that ArsC forms a complex with arsenate (Liu and Rosen, 1997). This complex then interacts with GSH. Adding GSH directly to ArsC does not produce evidence of any interaction. A direct association between glutaredoxin and ArsC was also demonstrated (Liu and Rosen, 1997). The manner in which ArsC interacts with glutaredoxin is an important question to pose. Native ArsC does not have any tryptophan. Mutating the enzyme and placing a tryptophan residue near the active site would allow for fluorescence studies to be performed on the interaction between ArsC and Grx-1. The problem lies in the fact that Grx-1 has a tryptophan present. A new approach must therefore be taken if fluorescence

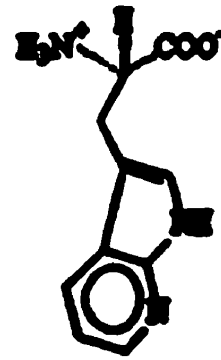
studies are to be applied. This technique involves the incorporation of tryptophan analogues, namely 7-azatryptophan, which have fluorescence properties different than normal tryptophan.

Fluorinated tryptophan analogues have already been used as probes for protein structural studies using  $^{19}\text{F}$  NMR in the 1970s (Sykes *et al.*, 1974). The use of tryptophan analogues as fluorescent probes was first suggested by Hudson in 1986 (Hudson *et al.*, 1986). Recent studies (Hogue and Szabo, 1993; Ross *et al.*, 1997) have demonstrated the usefulness of tryptophan analogues in studying protein-protein interactions. To incorporate Trp analogues, the host strain must not be able to synthesis Trp. The plasmid containing the ArsC gene under the control of a tight promoter is transformed into an auxotrophic strain of *E. coli* that cannot synthesis tryptophan. The bacteria can then be grown in minimal media supplemented with a reduced amount of tryptophan until a sufficient amount of cell mass has accumulated. The tryptophan analogues are then added, and the expression system is then induced. The result, when used with a tight promoter, is a high yield of the desired protein with the incorporated analog. Using this technique, a tryptophan analogue with a red-extended absorption spectrum (compared to normal Trp) can be used to selectively excite this desired Trp analogue in the presence of other tryptophan containing proteins, such as Grx-1. Figure 1-2 illustrates the structure of Trp and some of its analogues. The use of ArsC mutants containing tryptophan with the subsequent incorporation of tryptophan analogues would allow for the use of fluorescence spectroscopy to probe the interaction between ArsC and the Trp-containing Grx-1.

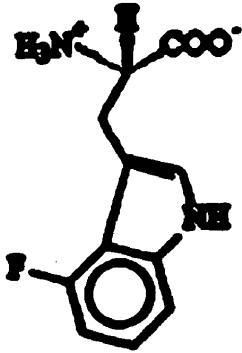
The complete structure of ArsC has not yet been determined. The initial step in elucidating a protein's structure is to determine its secondary structure. Several prediction programs exist which predict a protein's secondary structure based on natural tendencies



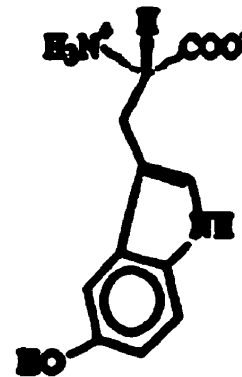
Tryptophan



7-Azatriptophan



4-Fluorotryptophan



5-Hydroxytryptophan

**Figure 1-2: Tryptophan and Tryptophan Analogs.** Chemical structure of tryptophan and various tryptophan analogs.

of individual residues and the influence of neighbouring residues within a protein. The first algorithm was devised by Chou and Fasman (Chou and Fasman, 1978). It predicts secondary structure based on the propensities of amino acids being included in specific secondary structures. Each amino acid carries secondary structural tendencies and probabilities of being included in specific secondary structural elements which are based on an examination of known protein structures. Individual amino acids are assigned as being included in specific secondary structure, as long as the probability within a range of amino acids is above 1.0 (Chou and Fasman, 1978). The process is used for the entire length of the protein and secondary structural content is assigned.

A second method used for secondary structure prediction is the nearest-neighbour Predict (nnPredict) method (Kneller *et al.*, 1990). This method uses a neural network to predict secondary structure. A neural network is an information-processing model inspired by the way the densely interconnected, parallel structure of the mammalian brain processes information. It is composed of a large number of highly interconnected processing elements that are analogous to neurons and are tied together with weighted connections that are analogous to synapses. The neural network incorporates network weights for every residue and elucidates their tendencies of being included in specific secondary structure based on the tendencies of neighbouring residues.

The Gibrat method aligns sequences of queried proteins with those of proteins whose structure is known and assigns secondary structural content based on the results of these comparisons with a database (Gibrat *et al.*, 1987). The Levin assigns secondary structures based on the premise that short, homologous sequences of amino acids have similar structural tendencies. Comparisons with the sequences of a known database are made and, consequently, secondary structural assignments are then made (Levin *et al.*,

1986). Another method, the DPM method, uses a combination of the Chou-Fasman method with the prediction of the class of the protein (Deleage and Roux, 1987). SOPMA, or self-optimized prediction method algorithm, uses multiple sequence alignments of the queried protein with those of proteins in a known database (Geourjeon and Deleage, 1995). The consensus method is actually a comparison between the above listed methods which yields a prediction based on the agreements between the Gibrat, Levin, DPM, and SOPMA methods. These methods can be found at [www.ibcp.fr/predict.html](http://www.ibcp.fr/predict.html).

Preliminary results using circular dichroism and structural prediction programs may help in elucidating the protein's structure. Circular dichroism is an experimental technique that helps to determine relative amounts of secondary structural content by exposing the protein to polarized light and comparing the difference in absorbance between left and right circularly polarized light at each wavelength. A plot of the ellipticity (difference in the absorbance of left circularly polarized light and right circularly polarized light) versus the wavelength yields a circular dichroism spectrum. By comparing the spectrum of a protein or polypeptide being studied to the spectrum of proteins and polypeptides whose secondary structure and circular dichroism spectra are known, one can use regression analysis programs to determine that protein's secondary structural content. There are numerous analysis programs, from simple multiple linear regression algorithms to the intricate SELCON program (Sreerama and Woody, 1993). Determination of the secondary structural content can be made using this experimental technique.

Circular dichroism can also be used to determine the melting temperature ( $T_m$ ) of a protein. The ellipticity can be monitored at a fixed wavelength while raising the

temperature to determine at which temperature the ellipticity and, hence, the protein's structure changes. By monitoring the ellipticity versus temperature, a melting curve is obtained. The mid-point of the melting curve is the melting temperature of the protein (Kahn *et al.*, 1992).

Determining the structure of ArsC and its interactions with its substrates, cofactors, and products allows for the elucidation of its enzymatic mechanism that is important due to the novelty exhibited by this reductase.



## **2. Materials and Methods**

### **2.1 Materials**

Solutions were made with distilled-deionized water. Liquids were handled with the aid of the appropriate Gilson Pipetmen (Models P2, P10, P20, P200, and P1000) purchased from Mandel Scientific Co Ltd. Mass determinations were carried out using either a Mettler AE50 or Mettler P1200N balance purchased from Fisher Scientific Inc. The temperature controlled water bath used was Model 1201 purchased from VWR Scientific. All electrophoresis experiments were carried out using a Power Pac 300 power supply, purchased from Biorad Laboratories. All pH measurements were determined using a Corning Model 240 pH meter from Corning Scientific Products. Photographs of agarose gels were taken using an MP-4+ Polaroid Camera System. SDS-PAGE gels were scanned using an Acer Prisa 310P scanner. All PCR experiments were carried out using a Cetus DNA Thermal Cycler from Perkin-Elmer. Centrifugations were carried out using one of the following centrifuges: model 59-A Micro-Centrifuge (Fisher Scientific), or a J2-HS centrifuge from Beckman fitted with either a JA-10, JA-14, or JA-20 rotor. Liquid chromatography experiments were performed using a Gilson Minipuls 2 peristaltic pump and a model 111B UV detector also from Gilson. Fractions were collected using a Frac-100 fraction collector purchased from Pharmacia Biotech. Bacterial cultures were grown in a model 3529 shaker-incubator purchased from Lab-Line Instruments, Inc. Circular dichroism experiments were carried out on an AVIV Model 62A DS circular dichroism spectrophotometer. Samples were placed in a 1 mm quartz cuvette purchased from Hellma Canada Ltd. UV-Vis spectra were performed on a Shimadzu UV-160 spectrophotometer. Fluorescence experiments were performed using

a SPEX Fluorolog Datamax 3000 fluorimeter. UV-Vis and fluorescence experiments were performed using 1 cm quartz cuvettes purchased from Hellma Canada Ltd.

Trizma Base, 3-(N-morpholino)propanesulfonate (MOPS), ethylenediaminetetraacetic acid (EDTA), ethidium bromide, agarose (type I-B), sodium dodecylsulfate (SDS), ammonium persulfate (APS), N,N,N',N'-tetraethylethylenediamine (TEMED),  $\lambda$  DNA markers (*EcoRI* / *HindIII*),  $\phi$ X174 DNA markers (*BsuRI* / *HaeIII*), glycine, ampicillin, kanamycin, isopropyl  $\beta$ -D-thiogalactopyranoside (IPTG), phenylmethylsulfonylfluoride (PMSF), and dithiothreitol (DTT) were all purchased from Sigma Chemical Company. Trypticase peptone, yeast extract, and select casamino acids were purchased from VWR scientific.  $\text{Na}_2\text{HPO}_4$ ,  $\text{KH}_2\text{PO}_4$ , NaCl, and KCl were purchased from BDH Chemical.

## 2.2 Methods

### 2.2.1 Polyacrylamide Electrophoresis

Discontinuous polyacrylamide electrophoresis was performed according to the method of Laemmli, 1970. 15% polyacrylamide slab gels were cast in groups of 4 using the Mighty Small<sup>TM</sup> minigel unit SE275 (Hoefer Scientific Instruments). A 30% stock solution of 37.5 : 1 acrylamide : bis-acrylamide (2.6% C) was purchased from Biorad Laboratories. The resolving gel was made by combining 20 mL of the 30% (w/v) stock acrylamide solution, 9.2 mL of dd-H<sub>2</sub>O, 10.0 mL of 1.5 M Tris (pH 8.8), and 0.4 mL of a 10% (w/v) SDS stock solution. Polymerization was initiated with the addition of 0.4 mL of a 10% (w/v) ammonium persulfate solution and 16  $\mu\text{L}$  of TEMED. The solution was then poured into the casting chamber and covered with a thin layer of water saturated *n*-

butanol. Polymerization was allowed to proceed for 40 minutes, after which the alcohol layer was decanted.

The stacking gel was prepared by mixing 3.4 mL of stock acrylamide, 2.5 mL of 1.0 M Tris (pH 6.8), 0.2 mL of 10 % SDS, 0.2 mL of a 0.1% (w/v) bromophenol blue solution, and 13.4 mL of dd-H<sub>2</sub>O. Polymerization was initiated with the addition of 0.2 mL of 10% APS and 10 µL of TEMED. The resolving gel solution was then layered on top of the stacking gel, a 10 or 15 well comb inserted to form wells, and the gels were allowed to polymerize for 15 minutes. The gels were then removed from the casting chamber and placed in a plastic bag to be stored at 4 °C until needed.

Small quantities of the protein samples to be analyzed (approximately 1 µg) were placed in a 1.5 mL microcentrifuge tube. An equal volume of 2 x sample buffer (stock solution consists of 1.0 mL of 10% SDS, 0.25 mL of 1.25 M Tris (pH 6.8), 0.25 mL 2-mercaptoethanol, 0.2 mL glycerol, 0.1 mL of a 0.1% bromophenol blue solution, and 0.7 mL of dd-H<sub>2</sub>O) was then added to each sample tube. Each sample, as well as an aliquot of SDS-7 standards, was then heat denatured at 95 °C for 3 minutes. A prepared slab gel was inserted into the electrophoresis unit and filled with electrophoresis buffer consisting of 194 mM glycine, 0.1 % SDS, and 25 mM Tris. The comb was then removed and each sample loaded into separate wells. Electrophoresis was performed at 110 V for 120 minutes. The slab gel was then removed from the unit and placed in a staining solution consisting of 0.1% Coomassie Blue-R, 50% methanol, and 10% glacial acetic acid and allowed to stain for 6 hours. The gel was then removed, rinsed, and placed in a destaining solution consisting of 50% methanol and 10% glacial acetic acid overnight. Destained gels were then scanned using an Acer scanner.

### 2.2.2 Agarose Electrophoresis

A 1X TBE running solution consisting of 0.09 M Tris-borate, 0.002 M EDTA, and 0.5 µg/mL of ethidium bromide was prepared. This solution was used to cast the gel and as the electrophoresis buffer. The appropriate amount of agarose was dissolved up in the 1X buffer by microwaving the solution for 1 minute. A homemade horizontal 10 x 8 cm mini submarine gel unit was used. The unit was prepared for casting by placing the comb and borders into the unit. The warm agarose solution (approximately 60 °C) was poured into the unit and allowed to cross-link for 40 minutes. The unit was filled with enough 1X TBE buffer to cover the gel. The comb and borders were then removed. All used running buffer and gels were decontaminated with 2.5 M HCl and 0.5 M KMnO<sub>4</sub> prior to disposal.

A stock solution of gel loading buffer was prepared consisting of 40% sucrose, 0.5% SDS, and 0.001% bromophenol blue. Either of the following two standards were used: *EcoRI / HindIII* digest of λ DNA (size ranging from 21 226 to 564 bp) or *BsuRI / HaeIII* digest of ΦX174 (ranging from 1350 to 118 bp). Approximately 1 µg of standard and a relatively similar amount of sample were dissolved up in 7 µL of gel loading buffer and 7 µL of 1X TBE. The gel was then run at 70 V for 80 minutes. The gel was then carefully removed and photographed using Polaroid 667 film, a transilluminator and the MP-4+ camera system. The exposure time used was typically 45 sec.

### 2.2.3 Isolation of *E. coli* ArsC and *E. coli* Glutaredoxin-1

#### 2.2.3.1 Overexpression and Purification of Wild-type *E. coli* ArsC

The expression systems of both ArsC and Glutaredoxin-1 (Grx-1) were the gift of Dr. Barry P. Rosen, Department of Biochemistry, Wayne State University School of Medicine, Detroit, MI. The *ArsC* gene was inserted into the *pUC18* plasmid carrying ampicillin resistance and transformed into the JM109 strain of *E. coli*. ArsC was purified by a modification of the procedure of Rosen *et al.*, (1991). 2L cultures of the JM109 strain of *E. coli* containing the *ArsC* gene were grown at 37 °C with constant shaking in 2 x YT medium (Miller, 1972) with 100 µg/mL ampicillin. When the absorbance reached 0.7 at 600 nm (usually 8-10 hours), the cells were induced with 0.45 mM IPTG and grown for an additional 3 hours. The cells were then collected by centrifugation in 500 mL Nalgene polycarbonate bottles spun at 4000 x g at 4 °C for 45 minutes. The cells were then resuspended in PBS buffer ( 11 mM Na<sub>2</sub>HPO<sub>4</sub>, 1.5 mM KH<sub>2</sub>PO<sub>4</sub>, 140 mM NaCl, and 2.65 mM KCl) at pH 7.5, re-spun for an additional 45 minutes, and the cell pellet was then frozen overnight at -20 °C. The pellet was then thawed and resuspended in 5 volumes per gram of cells in Buffer A (10 mM MOPS, 2 mM EDTA, 2 mM DTT adjusted to pH 7.5 with Trizma base). The cells were then lysed by single passage through a French pressure cell at 20 000 psi, followed by the immediate addition of 30 µg of PMSF (dissolved up in isopropyl alcohol). The solution was then centrifuged at 50 000 x g for 2 hours at 4 °C to remove unlysed cells and cellular membranes. The supernatant was then applied to a 2.5 cm x 30 cm column (Biorad Laboratories) packed with approximately 100 mL of Q-Sepharose anion exchanger (Sigma Chemical Co.) at a flow rate of 1 mL/min. The column was then washed with 3-4 bed volumes of Buffer A

to remove unbound protein. The column was then eluted with 800 mL of Buffer A containing a linear gradient of NaCl from 150 – 250 mM. Approximately eighty-five 8 mL fractions were collected using a Pharmacia Frac-100 and analyzed by electrophoresis (15% SDS-PAGE). The peak fractions containing the desired protein were concentrated to approximately 10 mL using an Amicon stir-cell concentrator (model 8050 fitted with a YM10 membrane, both from Amicon Inc.) and applied to a 2.6 x 90 cm column (Pharmacia Biotech) packed with 49 g of Sephadex G-50 superfine (Sigma Chemical Co.) equilibrated with Buffer A + 0.2 M NaCl at a flow rate of 0.2 mL/min. Approximately fifty 6 mL fractions were collected and analyzed by SDS-PAGE electrophoresis, and the peak fractions were concentrated to 2 mL using an Ultrafree-15 10 000 MWCO centrifugal filter unit (Millipore Corporation). The samples were then stored at 4 °C until needed.

#### 2.2.3.2 Overexpression and Purification of *E. coli* Grx-1

Glutaredoxin-1 (Grx-1) was purified according to the method of Bjoenberg and Holmgren (1991). A 2 L culture of *E. coli* strain N4830 possessing the glutaredoxin expression plasmid pAHOB1, which carries the Grx gene under the control of the  $\lambda P_L$  promoter, was grown with constant shaking at 25 °C in 2 x YT medium containing ampicillin at a concentration of 100  $\mu$ g/mL until an absorbance of 0.7 was reached at 600 nm (typically 14 – 16 hours). The temperature was then raised to 40 °C to induce the cells (inactivating the temperature sensitive cl857 repressor) and grown an additional 5 hours. The cells were then collected by centrifugation in 500 mL Nalgene bottles at 4000 x g for 45 minutes at 4 °C. The cells were washed once with PBS and the pellet was

stored overnight in a  $-20\text{ }^{\circ}\text{C}$  freezer. The cells were then thawed and resuspended in 5 volumes per gram of cells of Buffer A. The solution was then passed through a French press at 20 000 psi, after which 30  $\mu\text{g}$  of PMSF was then added. The sample was then centrifuged at 50 000  $\times$  g for 2 hours, and the supernatant applied to the same Q-Sepharose column as previously mentioned for ArsC. The column was then similarly washed and then eluted with 150 mL of Buffer A containing 0.2 M NaCl. The eluted protein was then concentrated down to 9 mL using the Amicon stir cell concentrator (fitted with a YM3 membrane) and applied to the same Sephadex G-50 column used for ArsC. Approximately fifty 6 mL fractions were collected and analyzed by SDS-PAGE electrophoresis. The purified Grx-1 was then stored as a lyophilized powder.

#### 2.2.4 Protein Assay

Protein concentration was determined by the method of Lowry *et al.*, (1951).

#### 2.2.5 Plasmid Isolation

The p*ArsC* plasmid (p*UC18* carrying the *ArsC* gene) was isolated using the FlexiPrep™ plasmid isolation kit from Pharmacia Biotech. A 10 mL culture of the JM109 strain of *E. coli* carrying the p*ArsC* gene were grown at  $37\text{ }^{\circ}\text{C}$  in 2  $\times$  YT until an absorbance of 0.7 at 600 nm was reached. Four 1.5 mL samples of the culture were spun down to pellet the cells. Each pellet was then resuspended in 200  $\mu\text{L}$  of Solution I of the kit by vortexing. The cells were then lysed with the addition of 200  $\mu\text{L}$  Solution II and gentle mixing. 200  $\mu\text{L}$  of Solution III was then added with gentle mixing. The mixture was then centrifuged in a microcentrifuge at full speed for 5 minutes at room

temperature. The supernatant was then transferred to a clean centrifuge tube, to which 420  $\mu$ L of isopropanol was added. The solution was allowed to stand for 10 minutes, after which time the tubes were spun at full speed for 10 minutes to pellet the plasmid DNA. The supernatant was then aspirated off and the tubes were then inverted to drain off the excess alcohol. 150  $\mu$ L of the Sephaglas™ FP slurry was then added to the plasmid pellet and the suspension was subsequently vortexed gently for 1 minute to dissolve the pellet. The mixture was then spun down at full speed for 15 seconds, and the supernatant removed. The Sephaglas pellet was then washed with 200  $\mu$ L of the Wash Buffer and vortexed gently to mix. The suspension was spun down at full speed for an additional 15 seconds and the supernatant removed. The pellet was then resuspended in 300  $\mu$ L of 70% ethanol and then centrifuged for 15 seconds at full speed. After removal of the alcohol, the pellet was then tapped gently to disperse the beads and allowed to air dry for 10 minutes. The bound DNA was eluted from the beads with 50  $\mu$ L of dd-H<sub>2</sub>O and spun down at full speed for 1 minute. The supernatants from the four tubes were then pooled together. The plasmid DNA was then further concentrated with ethanol precipitation and stored dry at 4 °C. The purity of the plasmid was determined using 1.0% agarose gel electrophoresis.

#### 2.2.6 Site-Directed Mutagenesis of *E. coli* ArsC

Two mutants of ArsC were created using the QuikChange™ Site-Directed Mutagenesis Kit purchased from Stratagene. One mutant was designed to change the Ala-11 codon (GCC) to Trp (TGG) and the other to change the Tyr-7 codon (TAT) to Trp



(TGG). The Ala-11 mutant was named A11W. The Tyr-7 mutant was named Y7W. A pair of primers was designed to be used with the Stratagene kit for each mutant.

#### 2.2.6.1 Primer Selection for the A11W Mutant of ArsC

The primers designed for the A11W mutation were prepared according to the guidelines outlined in the QuikChange™ Kit. The primers must be complementary to each other (including the complementary mutation from A-11 to Trp), anneal to the same sequence on opposite strands of the plasmid, and be between 25 to 45 bases in length. The desired mutation should be in the middle of the primer with 10-15 bases encompassing the mutation on both sides. The primers should have a GC content of at least 40%, terminate in either a G or C base (if possible), and have a minimum melting temperature of 78 °C according to the equation:

$$T_m = 81.5 + 0.41(\%GC) - (675 / N) - \% \text{ mismatch}$$

where N is the primer length in base pairs. The primers designed were designated PA11Wa for the first primer containing the Ala-11 to Trp mutation and PA11Wb for the complementary primer. The primers designed were 29 bp and had a predicted melting temperature of 82.3 °C for PA11Wa and 82.3 °C for PA11Wb. Both primers had a GC content of 58.6%. The primers designed are illustrated in Fig. 2-1 and were purchased from Oligos Etc.

```

acg ctg gcc gcg ctg gcg cta cgt ctc tct gtc aca ttg taa tga gat tct gat
      7                               11
M S N I T I Y H N P A C G T S R N T
atg agc aac atc act att tat cat aac cca gca tgc ggc acc tcg cgt aat acg

L E M I R N S G T E P T I I L Y L E
ctg gag atg atc cgc aac agc ggt acc gag ccg acc att att ctt tac ctt gaa

N P P S R D E L V K L I A D M G I S
aac ccg cct tcg agg gat gag ctg gtt aaa ctt att gcc gat atg ggt att tca

V R A L L R K N V E P Y E Q L G L A
gta cga gcg ctg ctg cgt aaa aac gtt gaa cct tac gag caa ctg ggt ctt gca

E D K F T D D Q L I D F M L Q H P I
gaa gat aaa ttt act gac gat cag ctc atc gac ttt atg ttg caa cac cca att

L I N R P I V V T P L G T R L C R P
ctg att aac cgt ccg atc gtg gtt acg ccg ctg gga acc aga ctg tgc cgt cct

S E V V L D I L Q D A Q K G A F T K
tct gaa gtg gtt ctg gat atc cta cag gat gcg cag aaa ggg gct ttc act aag

E D G E K V V D E A G K R L K
gaa gac ggt gaa aaa gtc gtt gat gaa gca gga aaa cgg ctg aaa taa ata ata

```

**Figure 2-1: Alignment of the primary sequence of *E. coli* ArsC with the ArsC gene displaying the A11W primer selection. The underlined region corresponds to the A11Wa primer for the A11W mutant. The boxed-in Ala-11 codon was mutated from GCC to TGG for the mutant protein. The A11Wb primer is the complementary oligonucleotide to the A11Wa primer (with the appropriate ACC codon encoding the Trp-11 mutation).**

### 2.2.6.2 Primer Selection for Y7W Mutant of ArsC

The primers for the Y7W mutant of ArsC were designed under the same scrutiny as those for the A11W mutant. The primers designed were designated PY7Wa for the first primer containing the Tyr-7 to Trp mutation and PY7Wb for the complementary primer. The PY7Wa and PY7Wb primers were 35 bp long and had a predicted melting temperature of 84.5 °C. The GC content of these primers was 54.2%. The primers designed are illustrated in Fig. 2-2 and were purchased from Oligos Etc.

### 2.2.6.3 Basic Protocol for Site-Directed Mutagenesis

All of the materials used for the amplification of the mutated plasmid (thin-walled PCR tubes and pipette tips) were autoclaved at 15 psi for 20 minutes on slow exhaust. Water used for the polymerase chain reaction segment of the mutagenesis was also similarly autoclaved. Upon receiving the primers, each was dissolved in enough sterile water to give a concentration of 100 ng/μL. For each mutant, a separate reaction tube was set up. Into each thin-walled microcentrifuge tube were aliquoted 5 μL of the 10 x reaction buffer (100 mM KCl, 100 mM [NH<sub>4</sub>]<sub>2</sub>SO<sub>4</sub>, 200 mM Tris-HCl, pH 8.8, 20 mM MgSO<sub>4</sub>, 1% Triton™ X-100, and 1 mg/mL BSA), 10 ng of parent plasmid (2 μL of a 5 ng/μL stock solution of isolated p*ArsC* plasmid-concentration determined from the ratio of 50 μg of dsDNA has an absorbance of 1.00 at 260 nm), 1.25 μL (125 ng) of primer #1, 1.25 μL of primer #2, 1 μL of dNTP mix, and 38.5 μL of sterile dd-H<sub>2</sub>O. The final reagent added was 1 μL of the *Pfu* DNA polymerase (2.5 U/μL) for a final volume of 50 μL. The reaction was then overlaid with 30 μL of mineral oil. The control reaction conditions are as follows: into a separate thin-walled microcentrifuge tube are added 5

```

acg ctg gcc gcg ctg gcg cta cgt ctc tct gtc aca ttg taa tga gat tct gat
  N  S  N  I  T  I  Y7  E  N  P  A11  C  G  T  S  R  N  T
atg agc aac atc act att tac cat aac cca gcc tgc ggc acc tcg cgt aat acg

  L  E  N  I  R  N  S  G  T  E  P  T  I  I  L  Y  L  E
ctg gag atg atc cgc aac agc ggt acc gag ccg acc att att ctt tac ctt gaa

  N  P  P  S  R  D  E  L  V  K  L  I  A  D  N  G  I  S
aac ccg cct tcg agg gat gag ctg gtt aaa ctt att gcc gat atg ggt att tca

  V  R  A  L  L  R  K  N  V  E  P  Y  E  Q  L  G  L  A
gta cga gcg ctg ctg cgt aaa aac gtt gaa cct tac gag caa ctg ggt ctt gca

  E  D  K  F  T  D  D  Q  L  I  D  F  M  L  Q  E  P  I
gaa gat aaa ttt act gac gat cag ctc atc gac ttt atg ttg caa cac cca att

  L  I  N  R  P  I  V  V  T  P  L  G  T  R  L  C  R  P
ctg att aac cgt ccg atc gtg gtt acg ccg ctg gga acc aga ctg tgc cgt cct

  S  E  V  V  L  D  I  L  Q  D  A  Q  K  G  A  F  T  K
tct gaa gtg gtt ctg gat atc cta cag gat gcg cag aaa ggg gct ttc act aag

  E  D  G  E  K  V  V  D  E  A  G  K  R  L  K
gaa gac ggt gaa aaa gtc gtt gat gaa gca gga aaa cgg ctg aaa taa ata ata

```

**Figure 2-2: Alignment of the primary sequence of *E. coli* ArsC with the ArsC gene displaying the Y7W primer selection. The underlined region corresponds to the Y7Wa primer for the Y7W mutant. The boxed-in Tyr-7 codon was mutated from TAT to TGG for the mutant protein. The Y7Wb primer is the complementary oligonucleotide to the Y7Wa primer (with the appropriate ACC codon encoding the Trp-7 mutation).**

$\mu\text{L}$  of the 10x reaction buffer, 2  $\mu\text{L}$  (10ng) of pWhitescript™ 4.5-kb control plasmid (5 ng/ $\mu\text{L}$ ), 1.25  $\mu\text{L}$  (125ng) of oligonucleotide control primer #1, 1.25  $\mu\text{L}$  (125 ng) of oligonucleotide control primer #2, 1  $\mu\text{L}$  of the dNTP mix, and 38.5  $\mu\text{L}$  of dd-H<sub>2</sub>O. The final addition is 1  $\mu\text{L}$  of the *Pfu* DNA polymerase for a final volume of 50  $\mu\text{L}$  and the entire reaction is overlaid with 30  $\mu\text{L}$  of mineral oil. All of the reagents used are supplied as part of the mutagenesis kit except for the parent plasmid (pA<sub>rs</sub>C) and the primers used for the mutations (A11Wa & A11Wb for the A11W mutant, and Y7Wa & Y7Wb for the Y7W mutant).

The cycling parameters used for amplification of the mutant plasmid are listed in Table 2-1. After temperature cycling was complete, the reaction was placed on ice to cool the reaction to below 37 °C. The next step is the addition of 1  $\mu\text{L}$  of *Dpn*I restriction enzyme (10 U/ $\mu\text{L}$ ) directly to the reaction mixture below the mineral oil overlay. The solution was then mixed gently by pipetting up and down. The mixture was then centrifuged in a microcentrifuge at full speed for 1 minute and placed in a water bath at 37 °C for 1 hour to digest the parental plasmid.

The mutated plasmid was then transformed into the *E. coli* XL1-Blue supercompetent cells that are supplied as part of the kit according to the following procedure. The *E. coli* cells were gently thawed from -80 °C on ice. 50  $\mu\text{L}$  of the thawed cells were aliquoted into each of three 1.5 mL pre-chilled microcentrifuge tube using sterile technique, one for each mutant and one for the control. 1  $\mu\text{L}$  of each of the *Dpn*I treated reaction mixture was then carefully transferred to the properly labeled aliquot of supercompetent cells. Each tube was swirled gently to mix and incubated on ice for 30 minutes. The cells were then heat shocked at 42 °C for 1 minute and then placed on ice for 5 minutes. 0.5 mL of

<u>Segment</u>	<u>Cycles</u>	<u>Temperature</u>	<u>Time</u>
1	1	95 °C	30 seconds
	16	95 °C	30 seconds
		55 °C	1 minute
		72 °C	7 minutes

**Table 2-1: PCR cycling parameters for the Quik-Change Site-Directed mutagenesis Kit.** The elongation time of 7 minutes was used as determined using the suggested guideline of 2 minutes per kbp of plasmid DNA.

sterile LB broth (pre-heated to 37 °C) was then added to each tube and the reaction mixture was incubated at 37 °C for 1 hour with gentle shaking. The two samples were plated onto separate LB agar plates containing 0.1 mg/mL ampicillin and incubated at 37 °C for 24 hours. Only 250 µL of the pWhitescript™ control reaction is plated onto an LB-ampicillin agar plate containing 20 µL of 10% (w/v) X-Gal (Sigma Chemical Co.) and 20 µL of 100 mM IPTG.

After 24 hours, 50 mL of 2 x YT media containing 0.1 mg/mL ampicillin was inoculated with one colony of each of the mutants from the LB agar plates. The separate cultures were grown to mid-log phase and the plasmid of each mutant was isolated using the previously described plasmid isolation kit. A 1.0% agarose gel was run to see if the plasmids were pure and the right size. Each mutated plasmid was stored as a 1 ng/µL solution at 4 °C in water until needed for transformation. The number of colonies of the control transformation was counted to deduce the mutagenesis efficiency of the pWhitescript™ plasmid. The expected colony number should be between 50 and 800 colonies for the control.

### 2.2.7 Bacterial Transformation

The general procedures for preparing competent cells and bacterial transformation were taken from Micklos and Freyer, (1990). Sterile technique was used throughout the procedure.

### 2.2.7.1 Procedure for Preparing Competent Cells

A 50 mL culture of LB medium was inoculated with *E. coli* strain W3110A33 (Trp auxotroph) and grown to mid-log phase (absorbance of 0.7 at 600 nm). Two 15 mL tubes were filled with 10 mL of mid-log phase cells. The tubes were spun down at 2500 rpm for 10 minutes, after which time the supernatant was sterilely poured off. To each tube was added 5 mL of sterile, ice-cold 50 mM CaCl<sub>2</sub>. The tubes were finger vortexed to resuspend the cells, and then incubated on ice for 20 minutes. After the incubation period, the tubes were spun down again at 2500 rpm for 5 minutes. The supernatant was carefully poured off, and 1 mL of fresh, sterile, ice-cold CaCl<sub>2</sub> was added to each pellet. The tubes were once again finger vortexed to resuspend the pellet, and then placed on ice for 24 hours.

### 2.2.7.2 Procedure for Transformation of Trp Auxotroph with pArsC Plasmid

Into two 15 mL tubes were placed 200 µL of competent W3110A33 cells. The tubes were then placed on ice. Into one tube was placed 10 µL (50 ng) of the isolated pArsC plasmid containing the A11W mutation and the tube labeled accordingly. Into the other tube was placed 10 µL (50 ng) of the isolated pArsC plasmid containing the Y7W mutation and the tube labeled accordingly. Both tubes were returned to the ice for a 20 minute incubation. Following the 20 minute incubation, the cells were heat shocked for 90 seconds at 42 °C and quickly returned to the ice bath for an additional 5 minutes. To each tube was then added 800 µL of sterile LB broth and the tubes were vortexed gently. The tubes were then placed in a shaking incubator at 37 °C for 2 hours to allow the cells to recover.



Following recovery incubation, 200  $\mu$ L of each cell suspension were spread onto separate LB-ampicillin agar plates properly labeled A11W and Y7W for each of the prepared mutants. A cell spreader was dipped in alcohol and flamed to ensure sterile technique. The plates were then allowed to stand to allow the cell suspension to soak into the LB agar. The plates were then incubated upside down for 24 hours at 37 °C. After the 24 hours of incubation, the cells were placed at 4 °C to retard growth of the transformed bacteria and also to slow the growth of any contaminating microbes.

One colony of each mutant was used to inoculate a 50 mL culture of LB media containing 0.1 mg/mL ampicillin and grown to mid-log phase. From these cultures glycerol stocks were made.

#### 2.2.8 Preparation of Glycerol Stocks

Cryo-vials (VWR Scientific) and 80% (v/v) glycerol solutions were autoclaved for 20 minutes at 15 psi to ensure sterility. Into each cryo-vial was added 900  $\mu$ L of mid-log phase cells (either A11W or Y7W mutant in the Trp auxotroph strain) and 100  $\mu$ L of sterile 80% glycerol. Care was taken to ensure sterile technique. Each vial was capped, gently agitated to mix, and finally placed at -80 °C until needed. Ten vials of each mutant were prepared.

#### 2.2.9 Incorporation of Trp Analogs Using M9 Medium

Each of the ArsC mutants was grown in M9 medium supplemented with the appropriate Trp analog after induction with IPTG. The M9 medium was prepared as follows: Into a 4 L baffled flask was added 40 g of casamino acids (VWR scientific), 30

mL of glycerol, and 1 mL of a 4 mg/mL solution of L-Trp all in a total volume of 1.8 L of dd-H<sub>2</sub>O. This solution was autoclaved for 20 minutes at 15 psi. 10 x M9 salts were prepared consisting of 67.82 g of Na<sub>2</sub>HPO<sub>4</sub>, 30 g of KH<sub>2</sub>PO<sub>4</sub>, 10 g NH<sub>4</sub>Cl, and 5 g of NaCl all dissolved up in 200 ml and autoclaved similarly. 4 mL of a 1 M MgSO<sub>4</sub> was prepared in a 15 mL tube and similarly autoclaved. Once cooled, the 10 x M9 salts, the MgSO<sub>4</sub>, and 200 mg of ampicillin were added sterilely to the 4 L flask. 200 μL of a 1 M CaCl<sub>2</sub> solution was prepared and sterile-filtered into the flask using a 0.22 μm filter (VWR Scientific). 200 μL of a 1% (w/v) vitamin B1 was also sterilely filtered into the flask. The solution was swirled to mix the components, after which the medium was inoculated with either the A11W or Y7W mutant. The culture was then grown with constant shaking at 37 °C until an absorbance of 1.2 was reached at 600 nm, typically 18-24 hours. To the culture was then added IPTG for a final concentration of 0.45 mM and 40 mg of the appropriate Trp analog (7-azatryptophan). The culture was then grown an additional 6 hours at 37 °C, after which time the cells were harvested by centrifugation in 500 mL Nalgene bottles spun at 4500 x g for 45 minutes. Growth of each of the mutants without incorporation of any Trp analog was done in 2 L of LB medium (with 0.1 mg/mL ampicillin) at 37 °C with induction at an absorbance of 0.7 at 600 nm using 0.45 mM IPTG. The cultures were then grown an additional 3 hours.

The cells were then processed in the same manner as for the wild-type ArsC. A11W ArsC and Y7W ArsC were then stored at 4 °C.

#### 2.2.10 Amino Acid Analysis of *E. coli* ArsC

Amino acid analysis of ArsC was performed according to the method of Bidlingmeyer

*et al.*, (1984), using the Waters Pico-Tag™ system (Millipore Corp.). Protein samples were digested in 60 x 100 mm acid-cleaned culture tubes using a vapour phase 6 N HCl with 1% phenol solution for 24 hours at 110 °C. The tubes were then removed and wiped clean. They were then placed in a fresh reaction vial and vacuum dried. The samples were then redried using 20 µL of a redrying solution consisting of a 2 : 2 : 1 ratio of methanol : water: TEA. The redried samples were then derivatized using 20 µL of a 7 : 1 : 1 : 1 solution of methanol : water : TEA : PITC and allowed to react for 20 minutes. The derivatized samples were then vacuum dried. 5 µL Pierce standards were also dried, redried, and derivatized along with the protein samples.

The derivatized samples were then reconstituted in 200 µL of sample diluent which contained 4.75 mM sodium orthophosphate and 5% ACN (v/v) at pH 7.4. The reconstituted samples were then injected onto a Waters Pico-Tag™ column installed in the Waters 600 multi-solvent delivery system with the 441 detector set at 254 nm. Column temperature was preset to 38 °C. Elution was performed using a two solvent delivery setup. Eluent A consisted of 0.14 molar sodium acetate trihydrate and 0.05% (v/v) TEA adjusted to pH 6.4 with HPLC-grade acetic acid. Eluent B consisted of a 60:40 mix of HPLC-grade ACN : Milli-Q™ water. Eluent A was filtered through a Millipore HA 0.45 µm filter, while eluent B was filtered using a Millipore HV 0.45 µm filter. Both eluents were sonicated under vacuum for 20 seconds and continuously sparged with helium gas prior to and during elution. The elution gradient conditions are listed in Table 2-2.

Time (min)	Flow Rate (mL/min)	Eluent A (%)	Eluent B (%)
0	1.0	100	0
10	1.0	54	46
10.3	1.0	0	100
12	1.0	0	100
12.5	1.5	0	100
13.3	1.5	0	100
13.5	1.5	100	0
21	1.5	100	0
21.5	1.0	100	0

**Table 2-2: Elution conditions used for amino acid analysis using the Pico-Tag™ System and the 441 Detector.**

### 2.2.11 Secondary Structure Prediction of *E. coli* ArsC

Three methods were used to predict the secondary structure of ArsC based on its primary structure. The secondary structure may be predicted by considering how physiochemical properties of amino acids affect their neighbouring residues and then conjecturing as to the probability of that residue being included in specific secondary structures.

The first method used was the Chou and Fasman scheme (Fasman, 1989), which predicts secondary structure based on the propensities of amino acids to be included in specific secondary structures (such as  $\alpha$ -helices). The basic algorithm is a C language program (Fasman, 1989) that inputs the primary sequence and outputs the probabilities of each amino acid's tendency to be included in a specific secondary structural element. By listing all of the probabilities of each residue being included in specific secondary structures and then considering groups of amino acids together, a general picture can be deduced using the Chou-Fasman algorithm.

The second method used for secondary structure prediction was the nearest-neighbour Predict method (nnpredict). The prediction algorithm is found at the website <http://www.cmpharm.ucsf.edu/~nomi/nnpredict.html>. This method uses a two-layer, feed-forward neural network that incorporates network weights for every residue (Kneller, *et al.*, 1990).

The final method used is actually a consensus of the Gibrat method, the Levin method, the DPM (double prediction method) method, and the self optimized prediction from alignments method. The Gibrat method aligns sequences of the protein being queried with sequences of proteins whose structure is known in a database (Gibrat *et al.*, 1987).

The Levin method uses the hypothesis that short homologous sequences of amino acids have the same secondary structure tendencies. Comparisons are then made with proteins of a database (Levin *et al.*, 1986). The DPM method uses the method of Chou-Fasman combined with the prediction of the class of the protein (Deleage and Roux, 1987). The SOPMA method uses multiple sequence alignments of the queried protein with those of proteins in a database to predict the secondary structure (Geourjeon and Deleage, 1995). The prediction method used to compare and contrast the above methods was termed the consensus method, which yielded a prediction based on the agreements between the Gibrat, Levin, DPM, and SOPMA methods. The above listed prediction methods can be found at the website <http://www.ibcp.fr/predict.html>.

#### 2.2.12 CD Spectroscopy

The CD instrument was calibrated using a 1 mg/mL solution of d-camphorsulfonic acid. A 6  $\mu$ M protein sample was used for all CD experiments with a buffer solution consisting of 36  $\mu$ M dithiothreitol (DTT), 1.2 mM sodium fluoride (NaF), 6  $\mu$ M ethylenediaminetetraacetic acid (EDTA), 1.0 mM Tris-Mops at pH 6.60. CD spectra were collected in the far-UV region from 240 nm to 190 nm, every nm with a 1.0 nm bandwidth at 20  $^{\circ}$ C for native protein. The averaging time at each wavelength was 20 seconds. The measured ellipticity was converted to mean residue ellipticity (M.R.E.) according to the equation (Yang *et al.*, 1986):

$$[\Theta]_l = (\Theta_{\text{obs}}) (10/cn)^{-1}$$

where  $[\Theta]_l$  is the final observed value for M.R.E. at wavelength  $l$ ,  $\Theta_{obs}$  is the initial value observed value (ellipticity),  $l$  is the path length in millimeters,  $c$  is the molar concentration, and  $n$  is the number of amino acids. The mean residue ellipticity values were used to plot the spectra and were then converted to  $\Delta E$  values for CD analysis algorithms according to the equation (Adler *et al.*, 1973):

$$[\Theta]_l = 3298 \Delta E$$

The secondary structure determinations were calculated using the SELCON program (Sreerama and Woody, 1993). In the SELCON program, first the proteins in the reference database are arranged in order of increasing root-mean-square difference from the CD spectrum to be analyzed. The spectrum of the proteins that are least like the protein to be analyzed are systematically eliminated, and an initial guess of the secondary structural content of the protein to be studied is made. The spectrum of the analyzed protein is then deconvoluted, *i.e.*, the spectrum is fitted to the spectrum of the remaining proteins in the database. The process is repeated until deconvolution ceases to yield a new estimate on the secondary structure (Greenfield, 1996).

### 2.2.13 Thermal Denaturations Of *E. coli* ArsC

Thermal denaturation data of ArsC protein was acquired at 222 nm on the AVIV spectropolarimeter. Protein concentration was 6  $\mu$ M and data was collected every 2  $^{\circ}$ C from 10 to 80  $^{\circ}$ C with a 5 minute equilibration time and a 20 second averaging time per data point. The melting temperature was narrowed down to between 40 and 60  $^{\circ}$ C and so complete spectra were taken from 240 to 190 nm every 2  $^{\circ}$ C from 36 to 60  $^{\circ}$ C. The

protein was then heated to 80 °C and a spectrum was taken, followed by cooling to 10 °C where a final spectrum was taken to be compared to the original spectrum. For all spectra run, the percentages of secondary structure were calculated using the SELCON program.

The transition temperature midpoint for the unfolding during thermal denaturation (melting temperatures) of the protein with arsenate, arsenite, and alone were calculated using the method described by Kahn, *et al.* (1992) by establishing an upper and lower baseline. The  $K_{eq}$  was calculated at each point as the distance to the lower baseline divided by the distance to the upper baseline. A van't Hoff plot of the  $\ln K_{eq}$  versus the  $1/T$  was used to interpolate from the point where  $\ln K_{eq} = 0$  to find the melting temperature ( $T_m$ ).

#### 2.2.14 Fluorescence Studies of *E. coli* ArsC

Fluorescence spectra were collected on a Spex 220 Fluorimeter configured at right angles with a slitwidth of 4 nm, unless otherwise stated. Excitation wavelength was set to 300 nm unless otherwise noted. The sample compartment was regulated at 20 °C. The emission spectra were collected from 320 nm to 450 nm with an increment of 1 nm and an integration time of 1 second. All spectra were baseline corrected.



## **Results**

### **3.1 Overexpression and Purification of Wild-Type *E. coli* ArsC**

The PMSF-treated cell lysate from a 2 L culture of ArsC was applied to a 2.5 x 30 cm Q-sepharose ion-exchange column at a rate of 1 mL/min. After washing with 3 - 4 bed volumes of buffer A, the column was eluted with a NaCl gradient of 0 to 200 mM and monitored at 280 nm with a Gilson 111B UV-detector. Figure 3-1 illustrates a typical elution profile for the Q-sepharose bound fractions. The fractions containing the ArsC (Peak A) were then concentrated down to approximately 10 mL and loaded onto a 95 x 2.6 cm Sephadex G-50 superfine column at a flow rate of 0.2 mL/min. The gel filtration elution profile is illustrated in Figure 3-2. Peak B contains the ArsC. The purification of wild-type ArsC yielded between 15 - 20 mg of protein per litre of culture. Once the protein was eluted off of the gel filtration column, the protein was more than 95% pure. The protein was then stored at 4 °C in 10 mM Tris, 200mM NaCl at pH 7.0 until used.

### **3.2 SDS-PAGE of Wild-Type *E. coli* ArsC**

The fractions containing the desired protein were verified using 15 % SDS-PAGE (Laemmli, 1970). The purity of the ArsC eluted off the gel filtration column is illustrated in Figure 3-3. The ArsC is seen as a single band corresponding to a molecular weight of 16 000 Daltons in lane 5 after staining with Coomassie Brilliant Blue. The molecular weight markers in lane 1 consist of: bovine serum albumin, 66 kDa; ovalbumin, 45 kDa; glyceraldehyde-3-phosphate, 36 kDa; carbonic anhydrase, 29 kDa; trypsinogen, 24 kDa; soybean trypsin inhibitor, 20 kDa;  $\alpha$ -lactalbumin, 14.2 kDa. Lanes 2 and 3 contain two

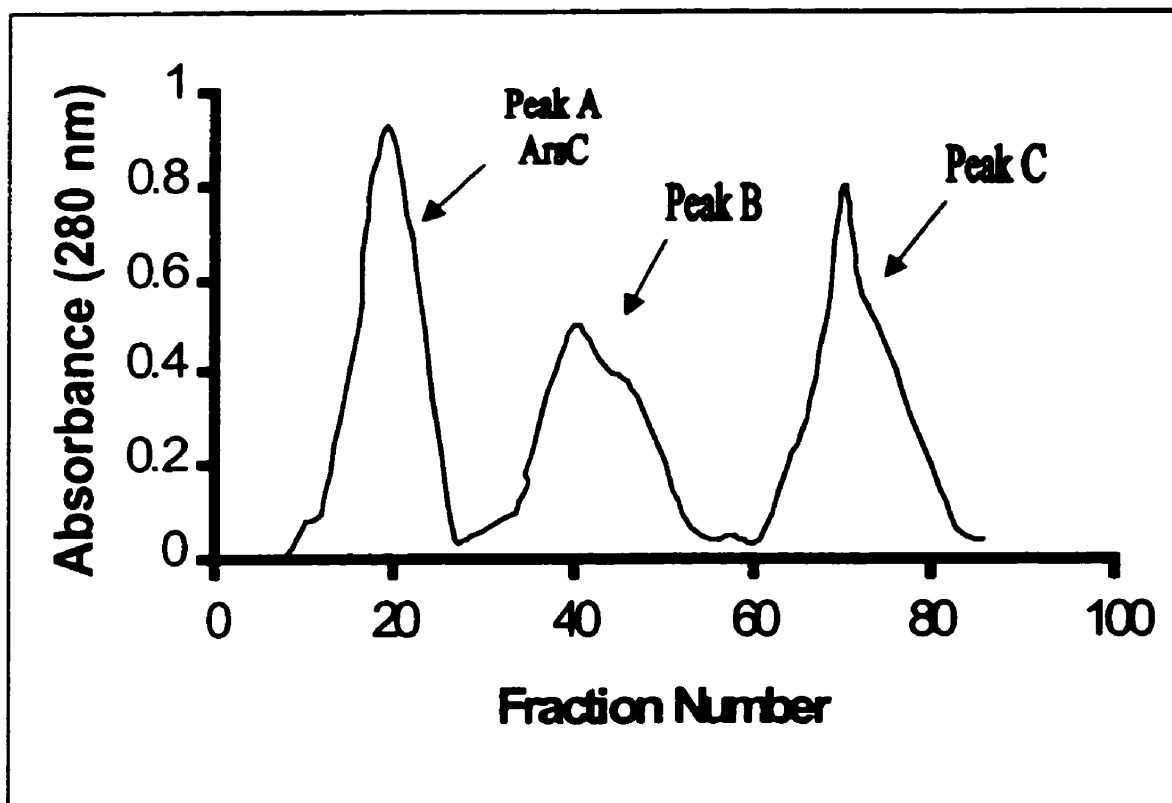


**Figure 3-1: Q-Sepharose ion exchange elution profile of *E. coli* ArsC.** The eluted proteins were monitored at 280 nm at a flow rate of 1 mL/min. The lysate was applied and washed with 3-4 bed volumes of buffer A (10 mM MOPS-Tris, 2 mM EDTA, 2 mM DTT, pH 7.5). The column was eluted with a linear salt gradient of 0 to 200 mM NaCl in buffer A. Peak A contained the ArsC.

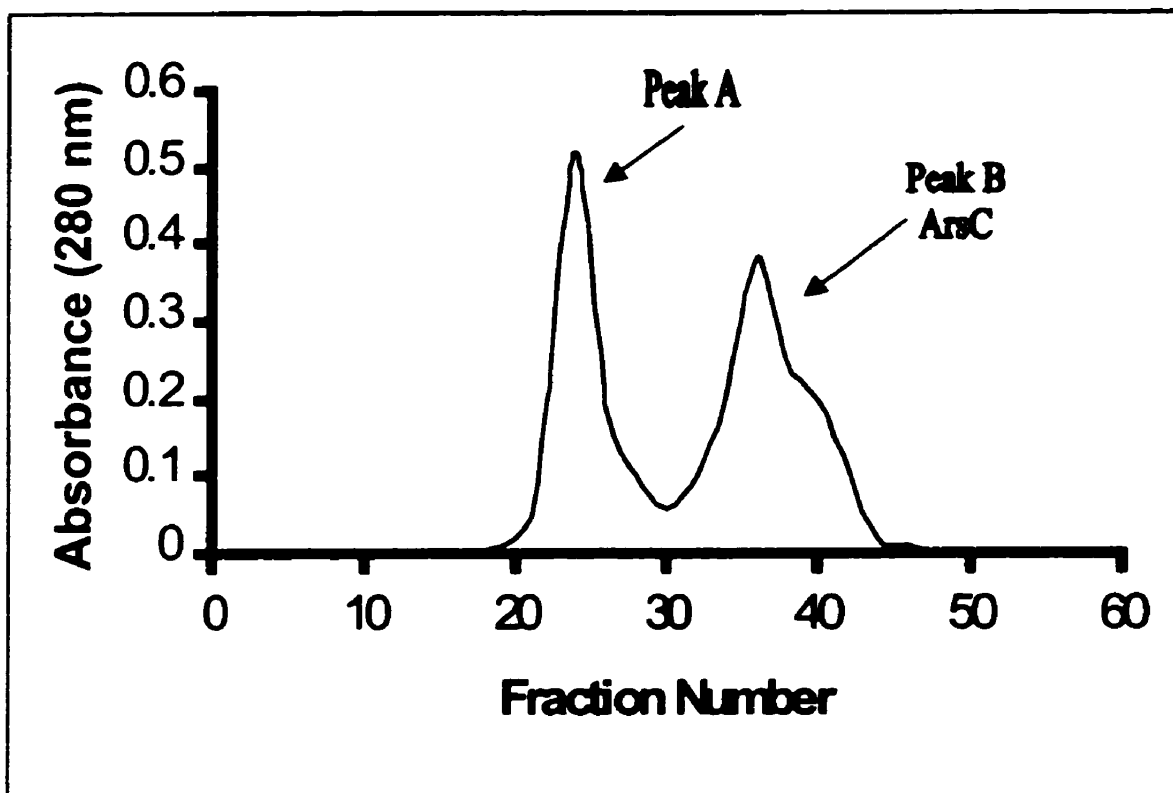


**Figure 3-2: Sephadex G-50 elution profile of *E. coli* ArsC.** The eluted proteins were monitored at 280 nm at a flow rate of 0.2 mL/min. The collected fractions containing ArsC eluted from Q-Sepharose were concentrated down to 10 mL and applied to the G-50 column. The column was then eluted with buffer A (10 mM MOPS-Tris, 2 mM EDTA, pH 7.5) containing 200 mM NaCl. Peak B contained the ArsC.

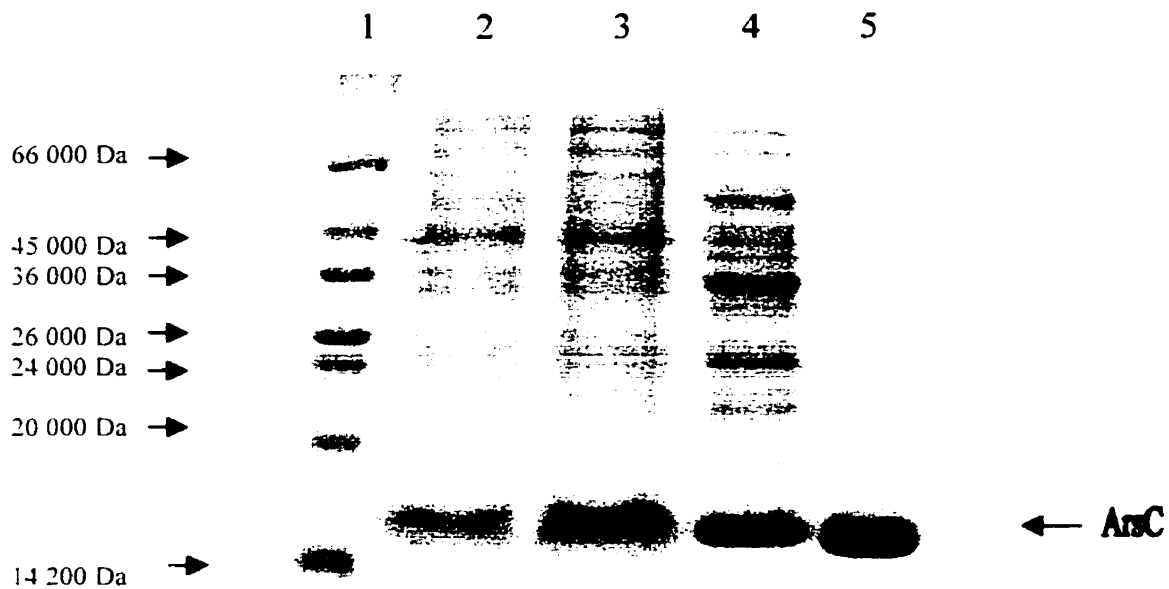


**Figure 3-3: 15 % SDS-PAGE of *E. coli* ArsC.** The first lane contains the molecular weight standards consisting of: BSA, 66 kDa; ovalbumin, 45 kDa; glyceraldehyde-3-phosphate, 36 kDa; carbonic anhydrase, 29 kDa; trypsinogen, 24 kDa; soybean trypsin inhibitor, 20 kDa; and  $\alpha$ -lactalbumin, 14.2 kDa. The second lane contains a sample of the cell lysate of the induced *pArsC*. The third lane is another sample of a different culture of *pArsC*. The fourth lane is a sample of the Q-sepharose bound fractions, Peak A. Lane 5 is a sample of the purified ArsC eluted off of the Sephadex G-50 column, Peak B. ArsC appears as a 16 kDa band.

separate samples of cell lysates of the induced bacteria carrying pArsC. Lane 4 contains a sample from Peak A of the Q-sepharose bound fraction. Lane 5 is a sample of Peak B of the Sephadex G-50 superfine eluted fractions.

### 3.3 Overexpression and Purification of *E. coli* Glutaredoxin-1

The cell lysate from a 2 L culture of the induced N4830 strain of *E. coli* carrying the pAHOB1 plasmid containing the Grx-1 gene was applied to a 2.5 x 30 cm Q-sepharose ion-exchange column at a rate of 1 mL/min. The column was then washed with 3-4 bed volumes of buffer A, followed by elution with buffer A plus 200 mM NaCl. The elution profile of the ion-exchange column is illustrated in Figure 3-4. The eluted fractions containing the Grx-1 (Peak A) were then concentrated down to approximately 10 mL and applied to a 95 x 2.6 cm Sephadex G-50 superfine column at a flow rate of 0.2 mL/min. The elution profile of the gel filtration column is illustrated in Figure 3-5. Peak B contained the essentially pure Grx-1 protein. Purification of wild-type *E. coli* Grx-1 yielded between 20 - 25 mg of protein per litre of culture. The protein was at least 95 % pure after elution off of the gel filtration column, as is illustrated in Figure 3-6. The purified protein was stored as a lyophilized powder at -20 °C until needed.

### 3.4 SDS-PAGE of *E. coli* Grx-1

The fractions containing the desired protein were verified using 15 % SDS-PAGE (Laemmli, 1970). The purity of Grx-1 eluted off the gel filtration column is illustrated in Figure 3-6. The Grx-1 is seen as a single band corresponding to a molecular weight of 10 000 Daltons in lane 5 after staining with Coomassie Brilliant Blue. The molecular

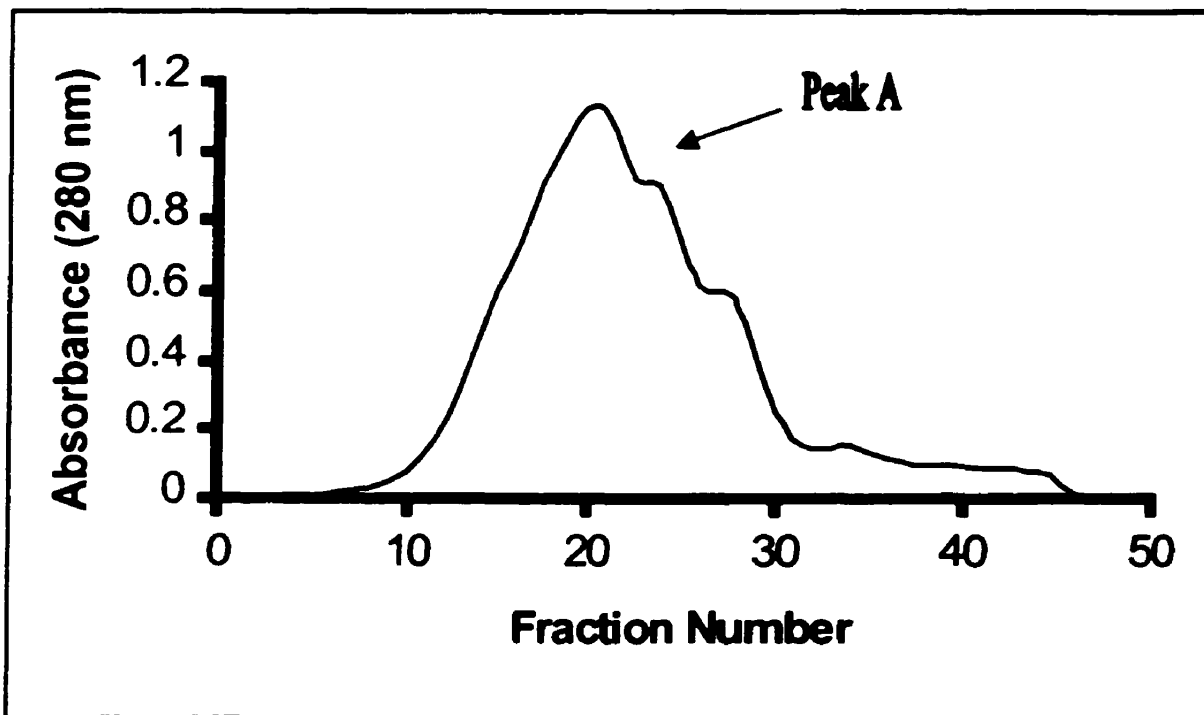


**Figure 3-4: Q-Sepharose ion exchange elution profile of *E. coli* Grx-1.** The eluted proteins were monitored at 280 nm at a flow rate of 1 mL/min. The lysate was applied and washed with 3-4 bed volumes of buffer A (10 mM MOPS-Tris, 2 mM EDTA, pH 7.5). The column was eluted with buffer A containing 200 mM NaCl. Peak A contained the Grx-1.

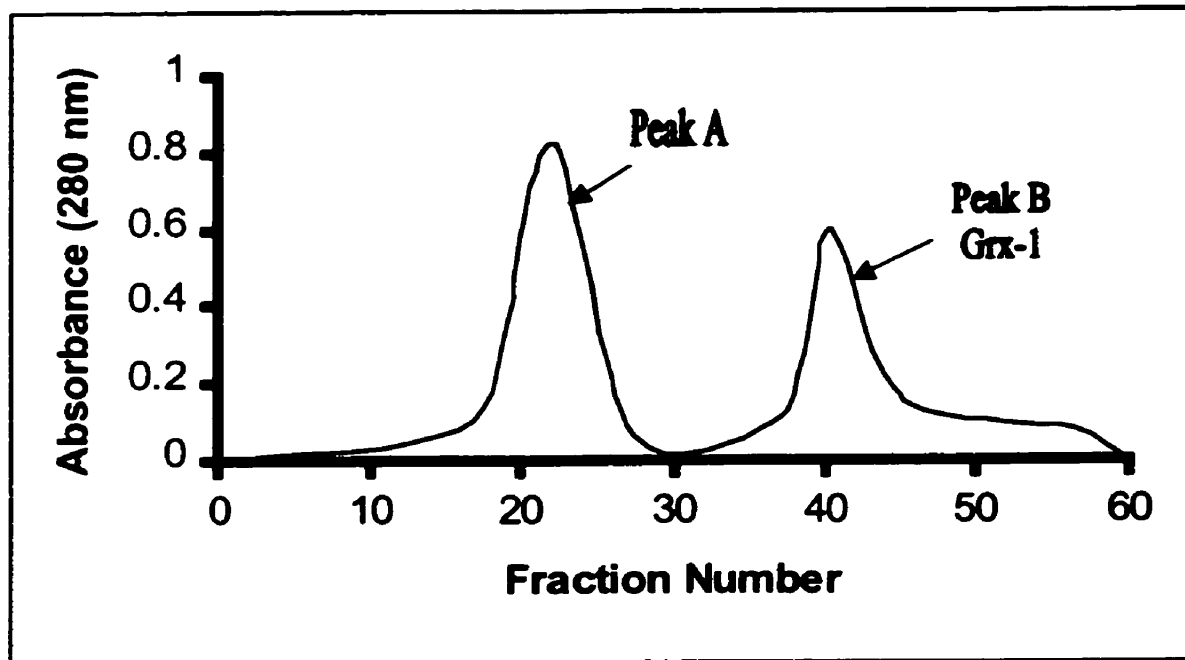


**Figure 3-5: Sephadex G-50 elution profile of *E. coli* Grx-1.** The eluted proteins were monitored at 280 nm at a flow rate of 0.2 mL/min. The collected fractions containing Grx-1 eluted from Q-Sepharose were concentrated down to 10 mL and applied to the Sephadex G-50 column. The column was eluted with buffer A (10 mM MOPS-Tris, 2 mM EDTA, pH 7.5) containing 200 mM NaCl. Peak B contains the Grx-1.

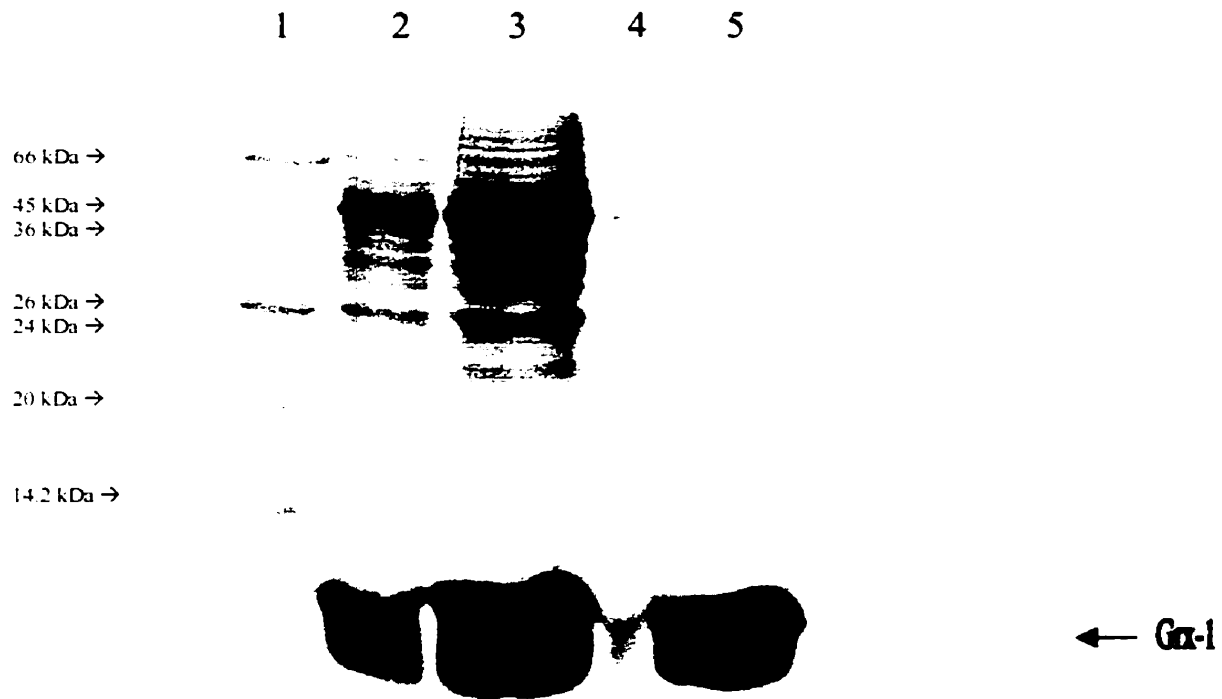


**Figure 3-6: 15% SDS-PAGE of *E. coli* Grx-1.** The first lane contains the molecular weight standards consisting of: BSA, 66 kDa; ovalbumin, 45 kDa; glyceraldehyde-3-phosphate, 36 kDa; carbonic anhydrase, 29 kDa; trypsinogen, 24 kDa; soybean trypsin inhibitor, 20 kDa; and  $\alpha$ -lactalbumin, 14.2 kDa. The second lane contains a sample of the cell lysate of the overexpressed Grx-1. The third lane is a sample of the Q-sepharose bound fractions of Grx-1 lysate. Lane 5 is a sample of Peak B eluted off of the Sephadex G-50 column. Grx-1 appears as a 10 kDa band.



weight markers in lane 1 consist of: bovine serum albumin, 66 kDa; ovalbumin, 45 kDa; glyceraldehyde-3-phosphate, 36 kDa; carbonic anhydrase, 29 kDa; trypsinogen, 24 kDa; soybean trypsin inhibitor, 20 kDa;  $\alpha$ -lactalbumin, 14.2 kDa. Lane 2 contains a sample of the cell lysate of the induced cells. Lane 3 contains a sample from Peak A eluted off of the Q-sepharose ion-exchange column.

### 3.5 Amino Acid Analysis of *E. coli* ArsC

Amino acid analysis of ArsC was used to confirm the identity of the protein and to determine the concentration. The hydrolyzed and derivatized ArsC samples were chromatographed on a Pico-Tag<sup>TM</sup> reverse-phase HPLC column, which is capable of resolving 17 amino acids as illustrated in Figure 3-7 (Bidlingmeyer *et al.*, 1984). Amino acids were quantified using response factors from external amino acid standards (Pierce Amino Acid Standard H). The ratios of detected amino acids are summarized in Table 3-1. The protein was confirmed to be ArsC using this method. The concentration of the ArsC used in circular dichroism experiments was determined to be 6  $\mu$ M. This was calculated using the molar ratios and picomole-quantity of alanine and phenylalanine detected in relation to the external Pierce standards that were used in the experiment. These amino acids were used because of their greater stability during acid hydrolysis. The greater accuracy provided by amino acid analysis was necessary for the calculation of mean residue ellipticities in circular dichroism experiments (Greenfield, 1996).



<b>Amino Acid</b>	<b>Expected Ratio</b>	<b>Obtained Ratio</b>
ASX	17	14.9 (15)
GLX	16	24.8 (25)
SER	6	5.3 (5)
GLY	8	8.1 (8)
HIS	2	1.8 (2)
ARG	9	9.7 (10)
THR	9	8.6 (9)
ALA	7	7.4 (7)
PRO	9	8.7 (9)
TYR	3	3.3 (3)
VAL	9	8.9 (9)
MET	4	3.9 (4)
CYS	2	1.7 (2)
ILE	13	12.3 (12)
LEU	16	15.7 (16)
PHE	3	3.1 (3)
LYS	8	8.2 (8)

**Table 3-1: Amino acid analysis of *E. coli* ArsC.** Expected ratio is the amino acid ratio determined according to the primary sequence of *E. coli* ArsC. Obtained ratio is the experimentally determined ratio using the Pico-Tag™ system. Number in parentheses is the rounded value. Asx is the sum of aspartic acid and asparagine. Glx is the sum of glutamic acid and glutamine. Tryptophan values are not listed because it is completely destroyed during acid hydrolysis.

### 3.6 Secondary Structure of *E. coli* ArsC

#### 3.6.1 Secondary Structure Prediction Using Algorithms

The predicted secondary structure of ArsC based on its primary structure using outlined algorithms is summarized in Table 3-2a and Table 3-2b. The nnPredict (Kneller *et al.*, 1990) and Gibrat (Gibrat *et al.*, 1987) algorithms do not calculate the relative amounts of turns in proteins. The Chou-Fasman algorithm (Fasman, 1989) predicts secondary structure by comparing the tendencies of the amino acids being included in specific secondary structures. The nnPredict method utilizes computational neural networks to predict secondary structures (Kneller *et al.*, 1990). The Gibrat method compares the influence of neighbouring sequences on the specific residues (Gibrat *et al.*, 1987). The Levin algorithm is similar to the Chou-Fasman scheme except that it compares 7-residue stretches of proteins (Levin *et al.*, 1986). The DPM method combines the Chou-Fasman algorithm with a class-prediction method (Deleage and Roux, 1987). The SOPMA method utilizes multiple alignments of protein segments with those in a database (Geourjon and Deleage, 1995). The consensus method is a combination of the consensus and the neural network methods.

All of the algorithms suggest that ArsC is mostly  $\alpha$ -helical in content with a smaller proportion of  $\beta$ -sheet. Note that the Chou-Fasman method (Fasman, 1989) tends to be more generous in predicting turns. It must also be noted that on average the prediction of secondary structure is at least 50 % accurate, since an average protein contains 27 %  $\alpha$ -helix and 22 %  $\beta$ -sheet (Voet and Voet, 1990). The predicted values tend to differ significantly between the methods. This may be due to the fact that the different methods

Residue No.	Amino Acid	Chou-Fasman	nnPredict	SOPMA
1	MET	B		
2	SER	B		T
3	ASN	B	B	T
4	ILE	B	B	
5	THR	B	B	B
6	ILE	B		B
7	TYR	B		B
8	HIS	B		H
9	ASN	T		
10	PRO	T		T
11	ALA			H
12	CYS			H
13	GLY	T		H
14	THR	T		H
15	SER	T		H
16	ARG	H		H
17	ASN	H		H
18	THR	H		B
19	LEU	H	H	B
20	GLU	H	H	B
21	MET	H	B	B
22	ILE	H	B	B
23	ARG	H	B	
24	ASN			
25	SER			
26	GLY			
27	THR	B		
28	GLU	B		
29	PRO	B		
30	THR	B	B	B
31	ILE	B	B	B
32	ILE	B	B	B
33	LEU	B	B	B
34	TYR	B	B	B
35	LEU			B
36	GLU			
37	ASN	T		
38	PRO	T		
39	PRO	T		
40	SER	H		
41	ARG	H		H
42	ASP	H		H
43	GLU	H	H	H
44	LEU	H	H	H
45	VAL	H	H	H
46	LYS	H	H	H
47	LEU	H	H	H
48	ILE	H	H	
49	ALA	H	H	H
50	ASP	H	H	H

51	MET	H	H	H
52	GLY		H	H
53	ILE		H	
54	SER	H	H	H
55	VAL	H	H	H
56	ARG	H	H	H
57	ALA	H	H	H
58	LEU	H	H	H
59	LEU	H		H
60	ARG	H		T
61	LYS			T
62	ASN			T
63	VAL			H
64	GLU	H		H
65	PRO	H		H
66	TYR	H	H	H
67	GLU	H	H	H
68	GLN	H	H	H
69	LEU	H	H	
70	GLY	H		
71	LEU	H		
72	ALA	H	H	
73	GLU	H	H	H
74	ASP	H		H
75	LYS	H		H
76	PHE	T		H
77	THR	T		H
78	ASP	H		H
79	ASP	H		H
80	GLN	H		H
81	LEU	H	H	H
82	ILE	H	H	H
83	ASP	H	H	H
84	PHE	H	H	H
85	MET	H	H	H
86	LEU		H	H
87	GLN	B		H
88	HIS	B		
89	PRO	B		
90	ILE	B		
91	LEU	B		
92	ILE			
93	ASN			T
94	ARG	B		B
95	PRO	B		B
96	ILE	B		B
97	VAL	B	B	B
98	VAL	B	B	B
99	THR	B		B
100	PRO	B		B
101	LEU	B		T
102	GLY	B		T

103	THR	B		T
104	ARG	B		B
105	LEU	B		H
106	CYS			
107	ARG			
108	PRO			
109	SER	B		H
110	GLU	B		H
111	VAL	B	H	B
112	VAL	B	B	B
113	LEU	B	H	B
114	ASP	H	H	H
115	ILE	H	H	H
116	LEU	H	H	H
117	GLN	H	H	H
118	ASP	H	H	H
119	ALA	H	H	H
120	GLN	H	H	H
121	LYS	H		H
122	GLY			T
123	ALA			T
124	PHE			T
125	THR	H		
126	LYS	H		
127	GLU	H		
128	ASP	H		
129	GLY	H		
130	GLU	H		
131	LYS	H	H	H
132	VAL	H	H	H
133	VAL	H	H	H
134	ASP	H	H	H
135	GLU	H	H	H
136	ALA	H	H	T
137	GLY	H	H	T
138	LYS	H	H	
139	ARG	H		
140	LEU	H		H
141	LYS			H

**Table 3-2a: Residue Assignments of the Secondary Structure Prediction of *E. coli* ArsC by various algorithms.** The Chou-Fasman values were determined according to the method of Fasman, 1989. nnPredict values were determined according to the method of Kneller *et al.*, 1990. The SOPMA method is described by Geourjon and Deleage, 1995. H = helix; B =  $\beta$ -sheet; and T = turns. Random coil is the assigned structure where no other structure is designated.

Method	$\alpha$ -Helix (%)	$\beta$ -sheet (%)	Turn (%)	Random Coil (%)
Chou-Fasman <sup>1</sup>	44.0	27.0	7.1	22.0
nnPredict <sup>2</sup>	33.3	9.9	-	56.7
SOPMA <sup>3</sup>	46.8	17.7	10.6	24.8
Gibrat <sup>4</sup>	51.1	17.0	-	31.9
Levin <sup>5</sup>	34.0	17.7	7.8	40.4
DPM <sup>6</sup>	24.1	21.3	10.6	44.4
Consensus*	39.0	12.1	0.7	48.2

**Table 3-2b: Secondary Structure Prediction of *E. coli* ArsC by various algorithms.** The Chou-Fasman<sup>1</sup> values were determined according to the method of Fasman, 1989. nnPredict<sup>2</sup> values were determined according to the method of Kneller *et al.*, 1990. Consensus\* is the agreement between the SOPMA<sup>3</sup> (Geourjon and Deleage, 1995), Gibrat<sup>4</sup> (Gibrat *et al.*, 1987), Levin<sup>5</sup> (Levin *et al.*, 1986), and DPM<sup>6</sup> (Deleage and Roux, 1987) methods. The calculation of the consensus\* value is described in Rost *et al.*, 1994. Note that the Gibrat and nnPredict methods do not include turns.



use slightly different criteria in determining the amino acids' propensities for being included in a given secondary structure. When combined with the influence of the neighbouring residues, these algorithms cannot take into account the complex interactions that occur between the polypeptide and its environment. These programs, therefore, serve only as a guide to a general picture and should not be taken as accurate determinations.

### 3.6.2 Circular Dichroism Studies of *E. coli* ArsC

For the native protein at 20 °C the circular dichroism spectra were obtained for: the protein alone (6 μM); with 60 μM arsenate; 300 μM arsenate; 60 μM arsenite; and 300 μM arsenite. The CD spectra of ribonuclease A was also taken as a control to illustrate the accuracy of the secondary structure calculation based on CD experiments. The results are summarized in Table 3-3. Note the discrepancies between the Chou-Fasman (C-F) estimates in secondary structure content in both RNase A and ArsC. The Chou-Fasman method over-estimated the helical content of RNase A by approximately 10% and underestimated the random coil content by 15%. Notice also that the secondary structures determined experimentally using CD were very accurate in predicting α-helical content and relatively accurate in predicting β-sheet. It was only possible to extend the scanning down to 190 nm because the instrument exceeded the threshold limit for acceptable values, which for the AVIV instrument was 600 dynode volts. The main reason for this is the use of Tris buffer in lieu of the suggested phosphate (Greenfield, 1996). Phosphate is an inhibitor of ArsC and, therefore, could not be used. Note also that the secondary

Sample	Method	$\alpha$ -helix	$\beta$ -sheet	Turns	R. Coil
RNase A	X-ray	0.240	0.330	0.140	0.290
	NMR	0.210	0.331	0.121	0.339
	C-F	0.323	0.387	0.137	0.153
	CD (1)	0.207	0.278	0.210	0.310
	CD (2)	0.240	0.272	0.250	0.230
ArsC	X-ray	ND	ND	ND	ND
	NMR	ND	ND	ND	ND
	C-F	0.440	0.270	0.071	0.220
	CD (1)	0.499	0.102	0.157	0.236
	CD (2)	0.495	0.117	0.198	0.186
ArsC with 10x Arsenate	X-ray	ND	ND	ND	ND
	NMR	ND	ND	ND	ND
	CD (1)	0.466	0.097	0.145	0.227
	CD (2)	0.465	0.115	0.195	0.186
ArsC with 50x Arsenate	X-ray	ND	ND	ND	ND
	NMR	ND	ND	ND	ND
	CD (1)	0.482	.0099	0.150	0.234
	CD (2)	0.480	0.116	0.199	0.189
ArsC with 10x Arsenite	X-ray	ND	ND	ND	ND
	NMR	ND	ND	ND	ND
	CD (1)	0.483	0.099	0.149	0.233
	CD (2)	0.478	0.113	0.191	0.183
ArsC with 50x Arsenite	X-ray	ND	ND	ND	ND
	NMR	ND	ND	ND	ND
	CD (1)	0.504	0.102	0.156	0.242
	CD (2)	0.500	0.120	0.196	0.190

**Table 3-3: Experimentally determined secondary structure of *E. coli* ArsC.** Structures determined using circular dichroism for ArsC alone, with arsenate, and with arsenite. The X-ray of RNase A was taken from Yang, *et al.*, 1986. The NMR structure of RNase A was taken from Rico *et al.*, 1991. CD (1) refers to the secondary structure calculated with the SELCON program using the Hennessey-Johnson reference database (Hennessey and Johnson, 1981). CD (2) refers to the secondary structure calculated with the SELCON program using the Kabsch-Sander reference database (Kabsch and Sander, 1983). C-F refers to the predicted content of secondary structures using the Chou-Fasman method (Chou and Fasman, 1978).

structure of ArsC did not change significantly with the addition of either substrate or product. Notice also that the secondary structure determined experimentally using CD for RNase A is fairly accurate compared to both the NMR and X-ray structures, suggesting that CD is a good method for the determination of secondary structural content of a protein. The NMR and X-ray structures of ArsC are not as of yet fully determined and, hence, cannot be compared. The secondary structure content was determined experimentally using the SELCON program (Sreerama and Woody, 1993). The ellipticity values measured by the AVIV instrument were first converted to mean residue ellipticities using the method described by Yang *et al.*, (1986). Mean residue ellipticities were then converted to  $\Delta E$  values according to Adler *et al.*, 1973, which are required by the SELCON program for the calculation of the estimated secondary structure of proteins (Sreerama and Woody, 1993). The secondary structure of ArsC was experimentally determined to contain approximately 49%  $\alpha$ -helix, 10%  $\beta$ -sheet, 15% turns, and 25% random coil (Table 3-3). There is a slight variance within the determined values when using the 2 different databases for calculating the secondary structure using the SELCON program. This is the major caveat of using this method for structural studies. The secondary structure of the proteins in the databases cause the calculations to be biased towards the proteins comprising the database. The Hennessey-Johnson database (Hennessey and Johnson, 1981) consists of 17 proteins and polypeptides including chymotrypsin, cytochrome c, myoglobin, and papain. The Kabsch-Sander database (Kabsch and Sander, 1983) consists of the same 17 proteins as the Hennessey-Johnson database. The difference between the two methods lies in the estimation of the secondary structural content of each protein or polypeptide. This is a common problem in

determining which residue is included in which secondary structure. There is no clear cut method to determine where one secondary structure ends and another begins. This problem is compounded by the fact that NMR structures do not always agree with X-ray crystallographic structures, as is evidenced in the case of RNase A in Table 3-3. This is the reason for the discrepancies in secondary structural content between different databases.

The program also tends to underestimate the quantity of  $\beta$ -sheet in proteins containing a high amount of this secondary structure when using current databases (Greenfield, 1996). A modern universal database that takes into account a variety of proteins whose secondary structural content is clearly defined is needed for better estimates of secondary structures.

### 3.6.3 Thermal Denaturations of *E. coli* ArsC

The melting curves of ArsC alone, with arsenate, and with arsenite are shown in Figure 3-8. Ellipticity was monitored at 222 nm with an averaging time of 20 seconds and a 5 minute equilibration time between temperature changes. The sigmoidal shape of the melting curves is indicative of a cooperative change in protein structure. The protein was considered to be in the native state before the transition and completely denatured after the transition state. Baselines were drawn for both the pre-transition and the post-transition states. The distance from the data point to the lower baseline divided by the distance from the data point to the upper baseline was taken to be the equilibrium

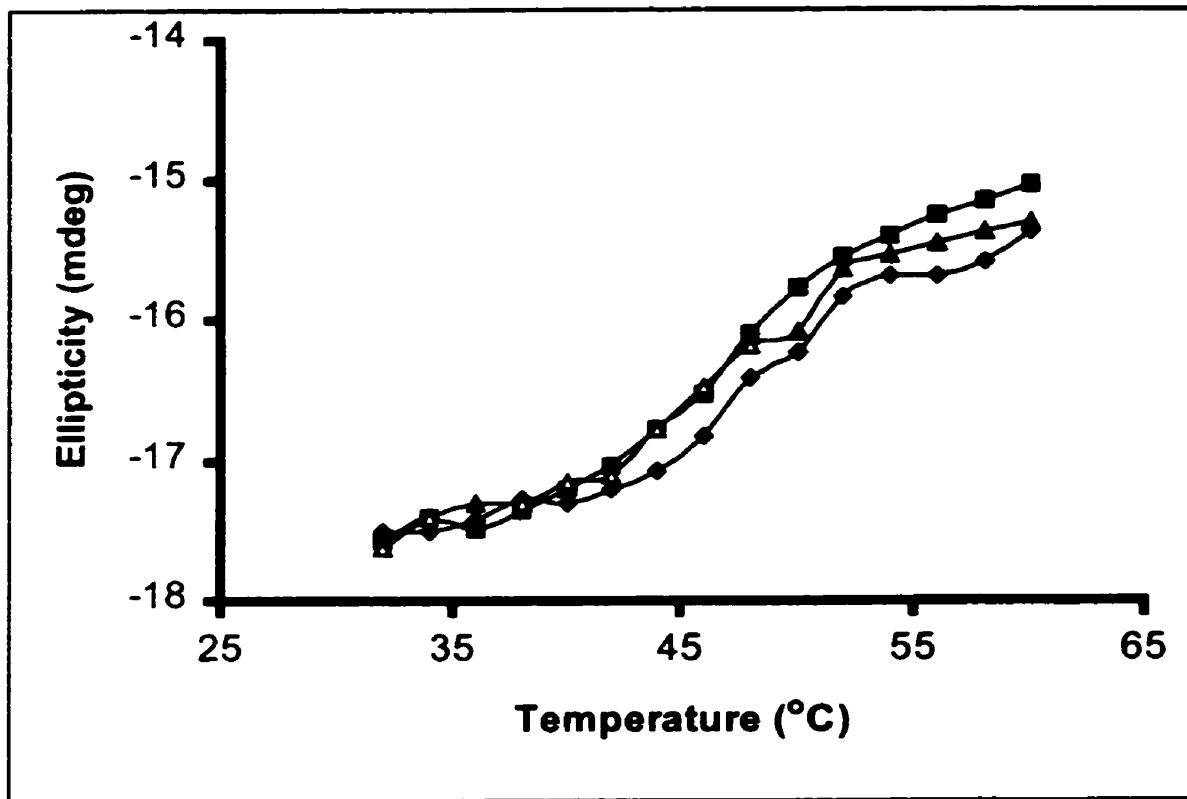


**Figure 3-8: Melting curves of *E. coli* ArsC.** The melting curves of ArsC were obtained using the AVIV CD spectrometer. The curve with the diamonds ( ● ) is indicative of the melting curve of ArsC without substrate or product. The curve with the triangles ( ▲ ) is the melting curve of ArsC with 50x arsenate. The curve with the squares ( ■ ) is the melting curve for ArsC with 50x arsenite. All melting curves were monitored at 222 nm with a 20 second averaging time and a 5 minute equilibration between temperatures.

constant ( $K_{eq}$ ). The melting temperature,  $T_m$ , was taken to be the interpolated point where  $K_{eq} = 0$  (Kahn *et al.*, 1992). The melting temperature, as determined using the van Hoff't plot to an accuracy of 5 °C (Kahn *et al.*, 1992), does not vary with the addition of substrate (arsenate) nor product (arsenite). The calculated values listed in Table 3-4 all hover around the 46 °C mark, which is well within the margin of error of the method used. The van Hoff't plots of ArsC alone, with arsenate, and with arsenite are illustrated in Figure 3-9. The melting temperature experiments are consistent with previous experiments which concluded that the secondary structure of ArsC did not change with the addition of either arsenate or arsenite. The CD spectra of ArsC were also collected from 240 - 190 nm at various temperatures, as shown in Figure 3-10.

### 3.7 Isolation of Plasmid R773

Isolation of the R773 plasmid containing the ArsC gene using the Pharmacia Flexi-Prep kit yielded between 5 - 10 ng of plasmid per millilitre of culture. The isolated plasmid was essentially free of genomic DNA, as can be seen in Figure 3-11. The band in lane 3 corresponds to the A11W mutated ArsC plasmid. A 1.0% agarose gel was used to identify and detect the purity of the isolated plasmid. The band in lane 4 corresponds to the Y7W plasmid. The extra bands above the expected band is due to the super-coiling of the isolated plasmids. Lane 1 contains the  $\lambda$  DNA / EcoRI + HindIII markers consisting of: a 21, 226 bp fragment; a 5148 bp fragment; a 4973 bp fragment; a 4268 bp fragment; a 3530 bp fragment; a 2027 bp fragment; a 1904 bp fragment; and 6 other smaller DNA fragments. The plasmids were stored in water at -20 °C until needed.

<b>Sample</b>	<b>T<sub>m</sub> (°C)</b>
<b>ArsC alone</b>	<b>45.9</b>
<b>ArsC with 50 x arsenate</b>	<b>46.6</b>
<b>ArsC with 50 x arsenite</b>	<b>46.4</b>

**Table 3-4: Experimentally determined melting temperatures of *E. coli* ArsC. ArsC alone refers to the protein without substrate or product. The second sample is ArsC with a 50-fold excess of its substrate (arsenate). The third value is determined for ArsC with a 50-fold excess of its product.**

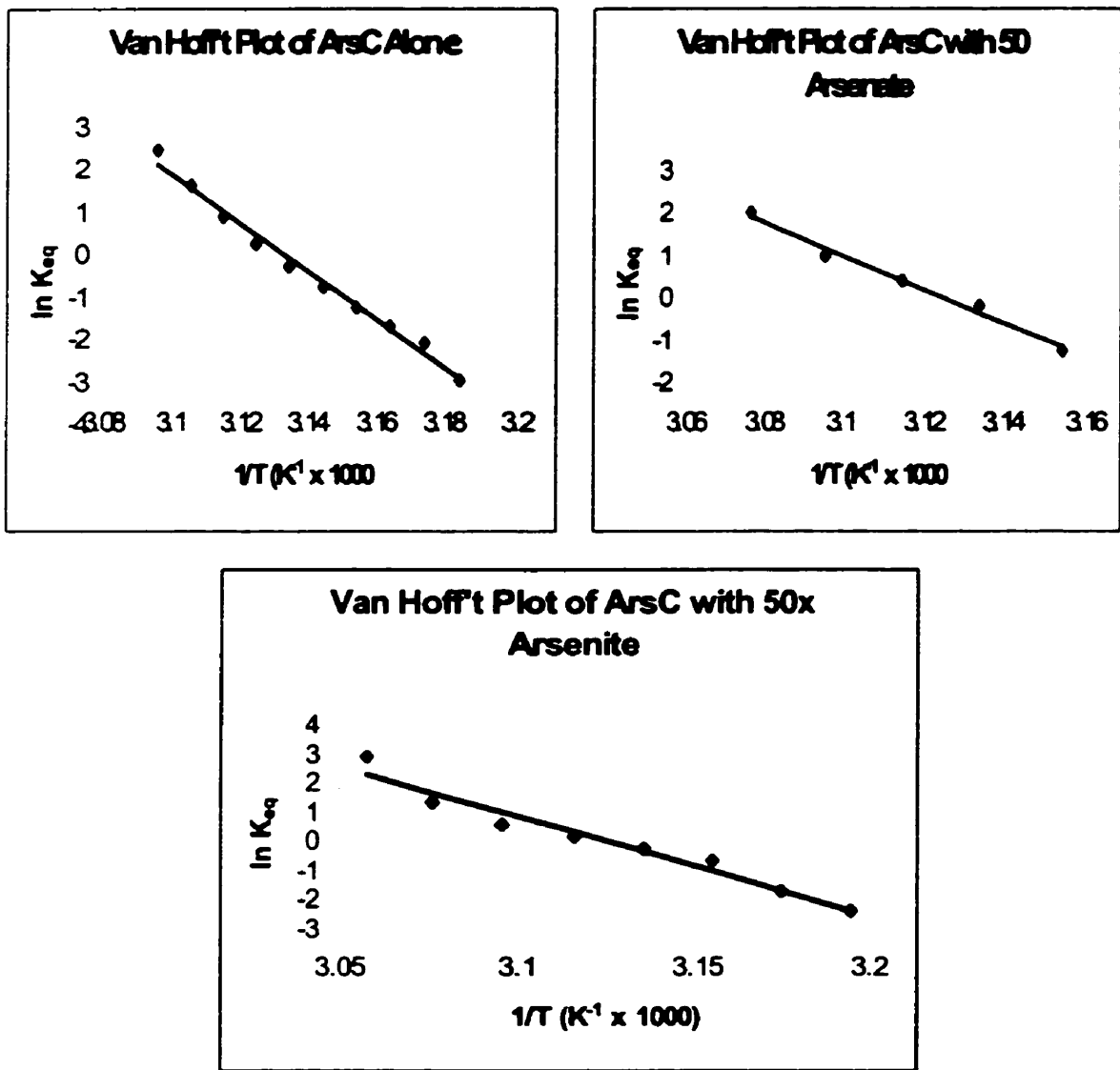


**Figure 3-9: Van Hoff't Plots of the temperature melts of *E. coli* ArsC.** The plot of  $\ln K_{eq}$  versus  $1/T$  of the ArsC samples were used to determine the melting points of ArsC with and without substrate or product. Linear regression was used to determine the line of best fit.



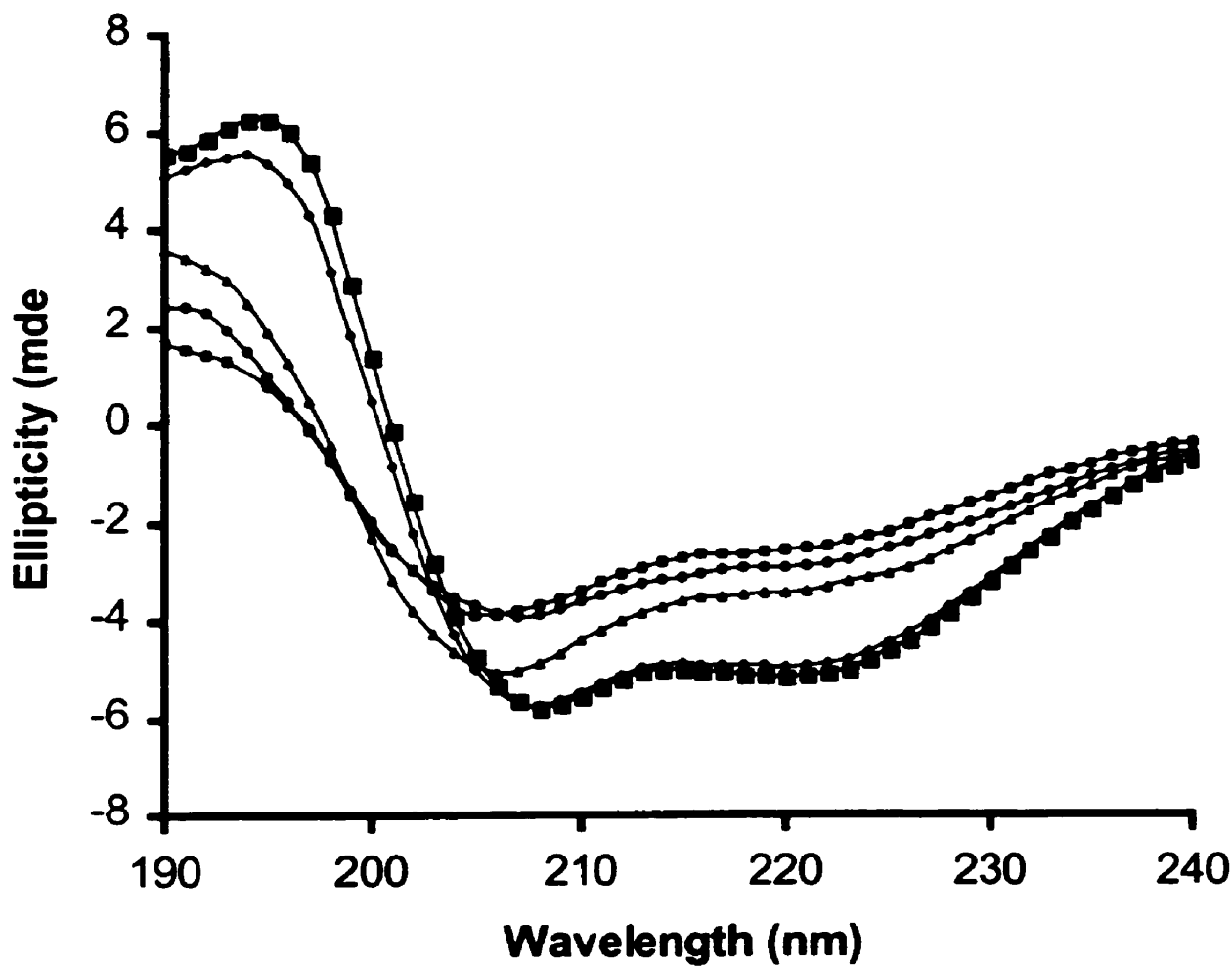


**Figure 3-10: CD spectra of *E. coli arsC* at various temperatures.** The scanned CD spectra of *arsC* were obtained using the AVIV CD spectrometer from 240 to 190 nm with an averaging time of 20 seconds and a 5 minute equilibration time between scans. The scans were taken at 20 °C (■); 36 °C (◆); 60 °C (▲); 80 °C (○); and cooled to 10 °C (□) after 80 °C.

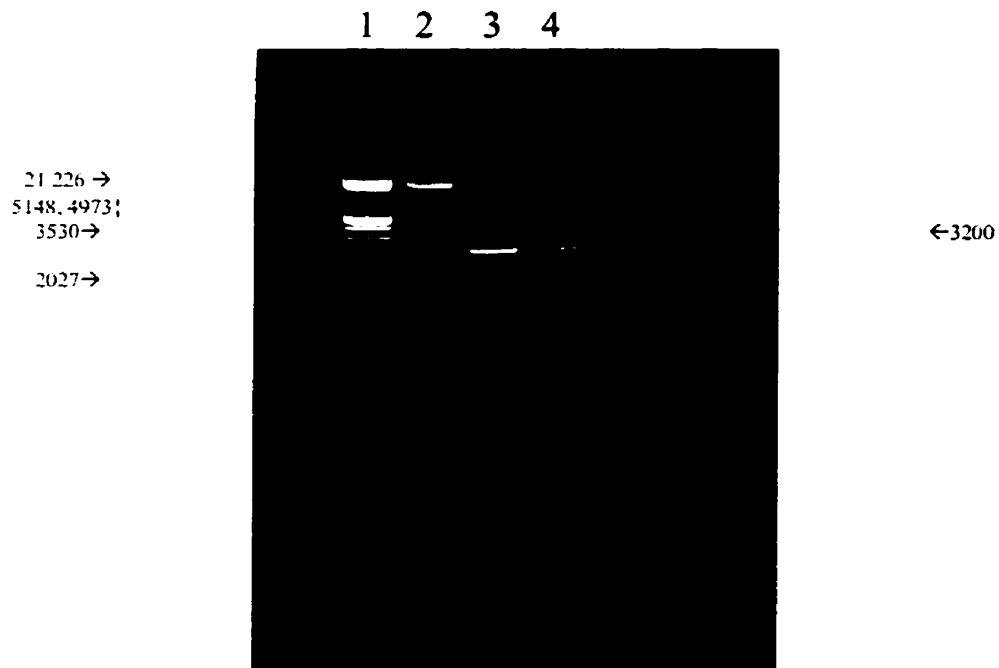


**Figure 3-11: 1.0% Agarose Gel of Purified pR773 plasmid containing the *E. coli* *ArsC* gene.** Lane 3 contains a sample of the isolated A11W mutant R773 plasmid, sized at 3200 bp. Lane 4 contains a sample of the isolated Y7W mutant R773 plasmid, similarly sized at 3200 bp. Lane 1 consists of  $\lambda$  DNA/*Eco*RI + *Hind*III markers consisting of: a 21, 226 bp fragment; a 5148 bp fragment; an 4973 bp fragment; a 4268 bp fragment; a 3530 bp fragment; 2027 bp fragment; 1904 bp fragment; and 6 other smaller fragments which ran off the gel. The sample in lane 2 is the isolated *pAHO81* plasmid carrying the *Grx-1* gene, sized at 4100 bp.

### **3.8 Transformation of Trp Auxotroph with A11W and Y7W Mutated *E. coli* ArsC**

The isolated A11W and Y7W pR773 mutant plasmids were transformed into the competent W3110A33 Trp auxotroph. Each mutant was then streaked onto LB-agar plates containing 50 µg/mL ampicillin for 24 hours. A 50 mL culture of LB medium was then inoculated with a single colony of each mutant and grown until an absorbance of 0.7 at 600 nm was reached. Glycerol stocks were made for each mutant and stored at -80 °C.

### **3.9 Isolation of ArsC A11W and Y7W Mutants**

The purification of mutated ArsC was the same as the procedure for the wild-type. The purity of each mutant was greater than 95 %, as can be seen in Figure 3-12. The yield of ArsC was between 10 - 15 mg for both mutants with the 7-azatryptophan analog grown in M9 minimal medium. Between 15 - 20 mg of protein per litre of culture was collected for each mutant when the mutants were grown in LB media (L-Trp). The proteins were stored at 4 °C in 10 mM Tris, 200 mM NaCl at pH 7.0 until needed.

### **3.10 Fluorescence Studies of *E. coli* ArsC Mutants with *E. coli* Grx-I**

#### **3.10.1 Fluorescence Emission Spectra of Mutant and Wild-Type *E. coli* ArsC**

The fluorescence emission spectra of wild type, A11W, and Y7W ArsC are presented in Figure 3-13. The excitation wavelength was 300 nm, selected because 7-azatryptophan fluoresces at this excitation wavelength whereas L-Trp does not (Ross *et al.*, 1997). The wild type protein does not exhibit any fluorescence, as is expected, since it does not contain any Trp residues. The A11W mutant exhibits an emission maximum of 366 nm,

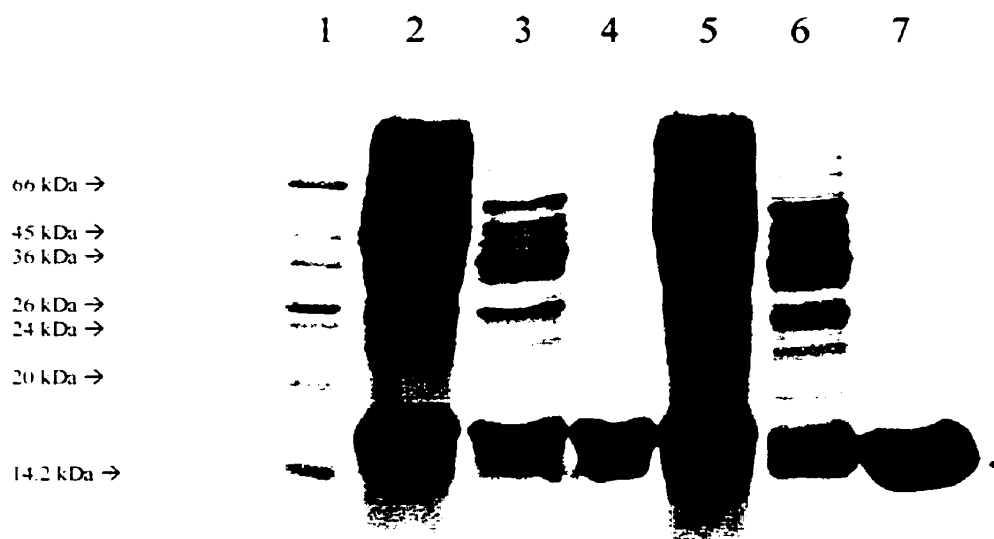


**Figure 3-12: 15% SDS-PAGE of the A11W and Y7W mutants of *E. coli* ArsC.** The first lane contains the molecular weight standards consisting of: BSA, 66 kDa; ovalbumin, 45 kDa; glyceraldehyde-3-phosphate, 36 kDa; carbonic anhydrase, 29 kDa; trypsinogen, 24 kDa; soybean trypsin inhibitor, 20 kDa; and  $\alpha$ -lactalbumin, 14.2 kDa. The second lane contains a sample of the cell lysate of the induced A11W mutant of ArsC. The third lane contains a sample of the Q-sepharose bound fraction of the A11W mutant. The fourth lane is a sample of the post Sephadex G-50 pure A11W mutant. The fifth lane is a sample of the cell lysate of the induce Y7W mutant of ArsC. The sixth lane contains a sample of the Q-sepharose bound fraction of the Y7W mutant. The seventh lane contains a sample of the pure post-Sephadex G-50 Y7W mutant. Both mutants of ArsC appears as a 16 kDa band.

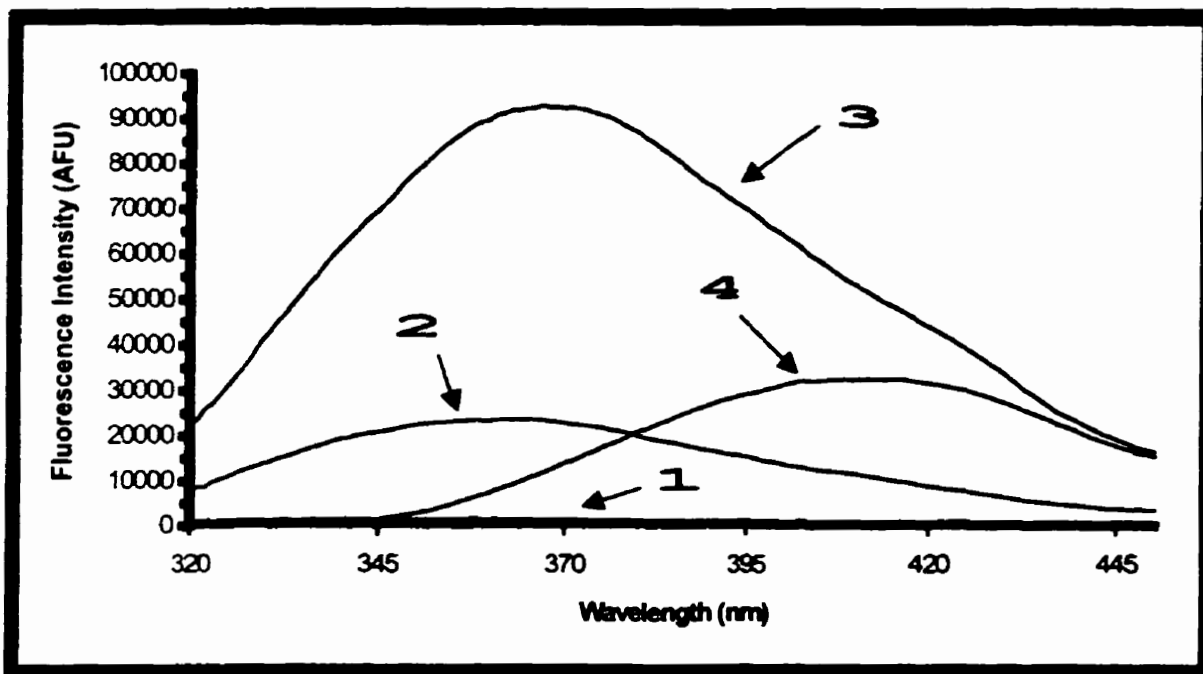


**Figure 3-13: Emission Spectra of wild type and Trp mutants of *E. coli* ArsC.** The excitation wavelength was 300 nm. Curve 1 is the wild type ArsC. Curve 2 is the A11W ArsC. Curve 3 is the Y7W ArsC. Curve 4 is the emission spectrum of free 7-azatryptophan. The concentration of each protein and the free amino acid was 2  $\mu$ M. All samples were prepared in 10 mM Tris, 200 mM NaCl, pH 7.0.

similar to the Y7W maximum of 367 nm. Free 7-azatryptophan displays an emission maximum of 412 nm when excited at 300 nm. These results indicate that the 7-azatryptophan of both mutants is relatively buried. The larger fluorescence intensity of the Y7W mutant is probably due to the fact that there is less quenching of the indole group compared to the A11W mutant. The quenching of the A11W mutant is probably due to the neighbouring Cys-12, since Cys is a potent quencher of Trp fluorescence (Lakowicz, 1986).

Although the emission spectra of both mutants indicate that the 7-azatryptophan is buried, the emission maxima of the two analog-incorporated mutants do not totally agree with the emission spectra of previous studies. Studies of the A11W and Y7W mutants with L-Trp indicate that the Y7W mutant is blue shifted relative to the A11W mutant (Liu and Rosen, 1997), indicating that the Y7W mutant is more buried. The emission maxima here are reported as 330 nm for the Y7W mutant and 350 nm for the A11W mutant when excited at 295 nm. Free L-Trp has an emission maximum of 354 nm when excited at 295 nm. This is probably due to the sensitive nature of the 7-azatryptophan (Ross *et al.*, 1997). Spectral properties of 7-azatryptophan are strongly affected by factors such as solvent accessibility, neighbouring residues, and proximity to quenchers.

### 3.10.2 Fluorescence Studies of 7AW-A11W ArsC with *E. coli* Grx-1

The fluorescence emission spectra of 7AW-A11W ArsC with various ligands are presented in Figure 3-14. The first curve is the emission spectrum of the 7AW-A11W protein alone in the buffer (10 mM Tris, 200 mM NaCl, pH 7.0). The second curve is the

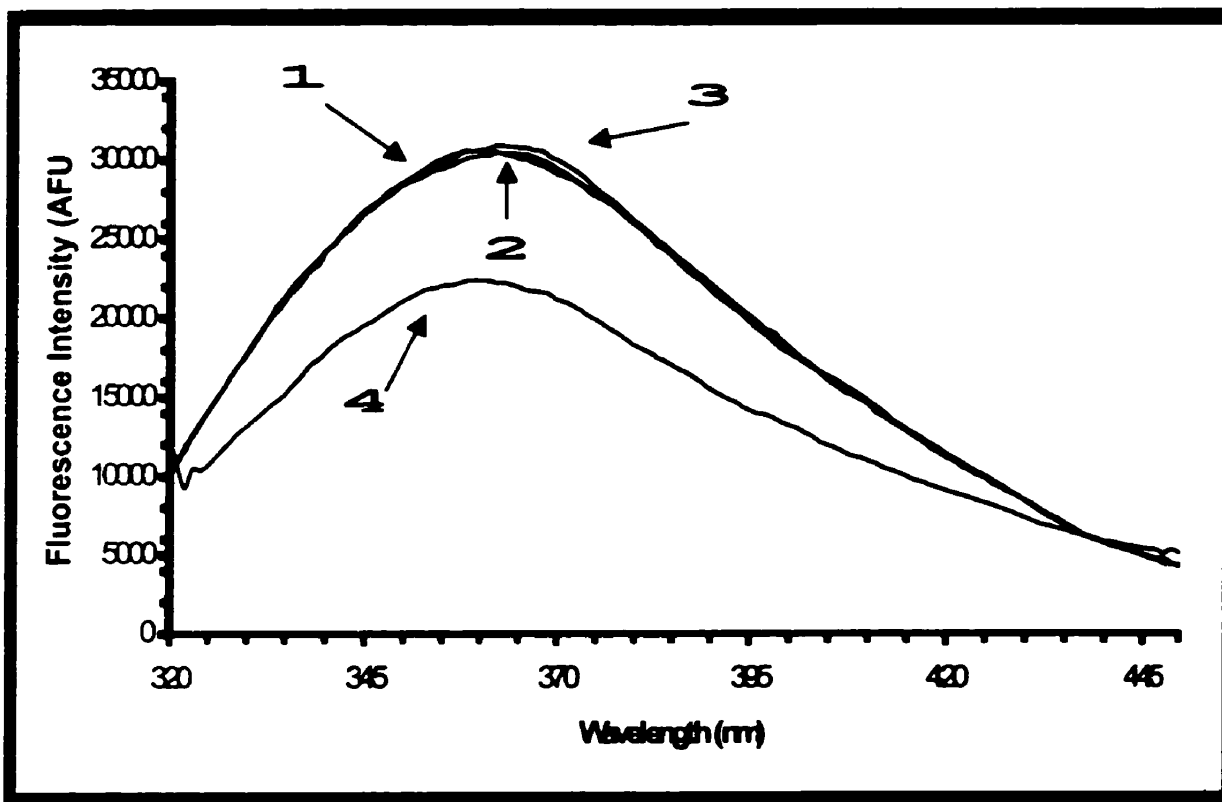


**Figure 3-14: Emission Spectra of the A11W *E. coli* ArsC mutant with various ligands.** Curve 1 is the emission spectrum of A11W ArsC. Curve 2 is the emission spectrum of A11W ArsC with 2  $\mu$ M Grx-1 added. Curve 3 is the previous sample with 2 mM arsenate added. Curve 4 is the previous sample with 0.5 mM glutathione added to the mix. The excitation wavelength was 300 nm, and ArsC concentration was 2  $\mu$ M. The spectra were corrected for dilution effects. All samples were prepared in 10 mM Tris, 200 mM NaCl, pH 7.0.

ArsC mutant with the addition of 2  $\mu\text{M}$  *E. coli* Grx-1. There is no change in either the fluorescence intensity or the emission maximum, suggesting that there is no interaction between the two proteins. There is also no change upon the addition of 2 mM arsenate (curve 3). The addition of 0.5 mM glutathione, however, induces a decrease in the fluorescence intensity of the A11W mutant (curve 4), suggesting some sort of interaction is occurring. The interaction may be due either directly to the glutathione or indirectly as the glutathione may reduce the Grx-1 which would then interact with the 7AW-A11W mutant. The former case was tested as GSH was added directly to a sample of the 7AW-A11W ArsC (Figure 3-15). The fluorescence intensity decreased with the addition of 0.5 mM GSH to 2  $\mu\text{M}$  of the 7AW-A11W mutant. The fluorescence intensity remained unchanged with the addition of 2  $\mu\text{M}$  Grx-1, indicating that the change in fluorescence was due directly to the GSH, and not the Grx-1. The reverse situation was also tested, *i.e.*, the addition of Grx-1 initially followed by the addition of GSH. These results supported the fact that the change in fluorescence was due to the addition of GSH, and not the addition of Grx-1.

### 3.10.3 Fluorescence Studies of 7AW-A11W ArsC with *E. coli* Grx-1

The fluorescence emission spectra of 7AW-Y7W ArsC with various ligands are presented in Figure 3-16. The first curve is a 2  $\mu\text{M}$  sample of 7AW-Y7W ArsC alone in 10 mM Tris, 200 mM NaCl, pH 7.0. The second curve is the preceding sample with 2  $\mu\text{M}$  *E. coli* Grx-1 added. The third sample is the previous sample with 2 mM arsenate added to the mix. The fourth curve is the preceding sample with 0.5 mM GSH added. As



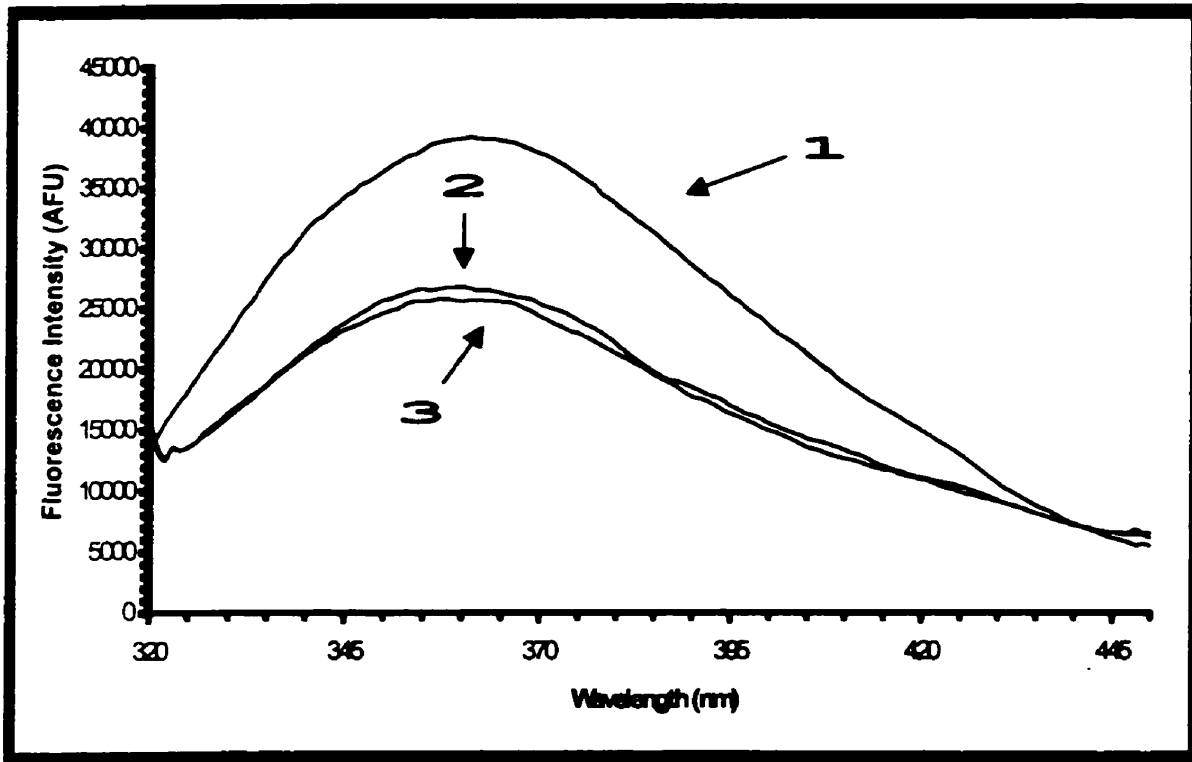


**Figure 3-15: Emission Spectra of the A11W *E. coli* ArsC mutant with GSH.** Curve 1 is the emission spectrum of 7AW-A11W ArsC alone. Curve 2 is the previous sample with the addition of 0.5 mM glutathione. Curve 3 is the 7AW-A11W ArsC containing 0.5 mM glutathione with the addition of 2  $\mu$ M Grx-1. The excitation wavelength was 300 nm, with a 7AW-A11W concentration of 2  $\mu$ M. All spectra were corrected for dilution effects. All samples were prepared in 10 mM Tris, 200 mM NaCl, pH 7.0.

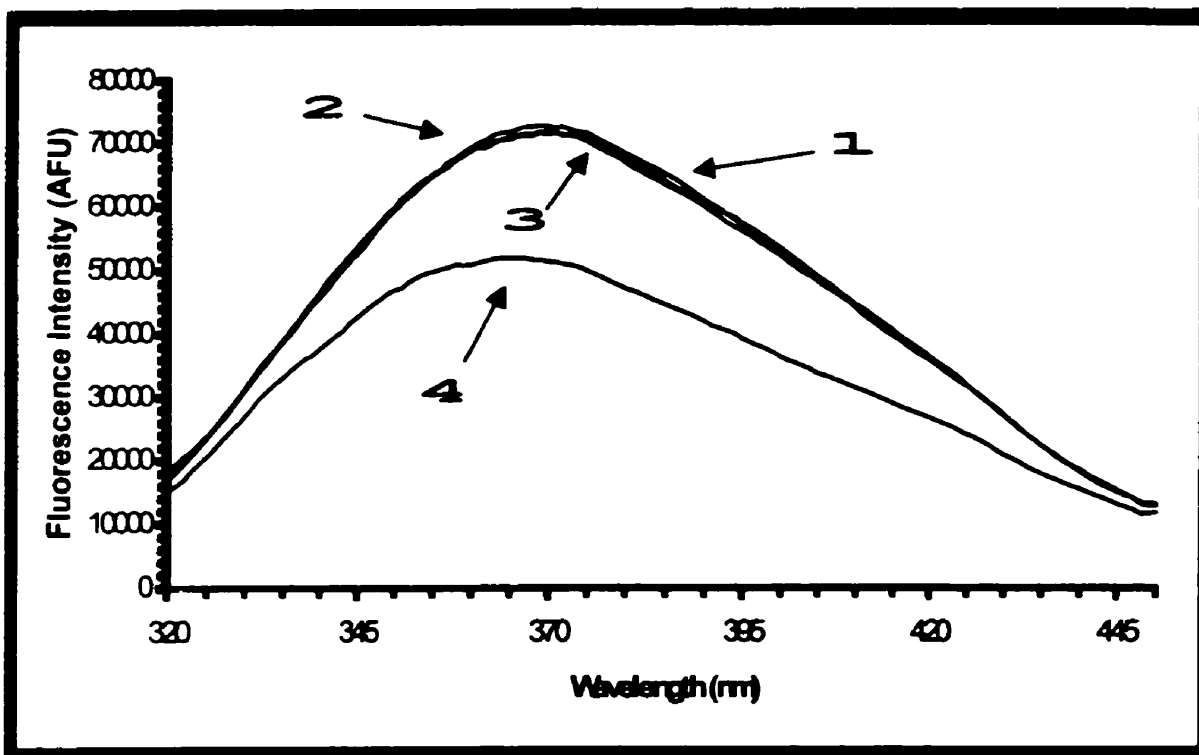


**Figure 3-16: Emission Spectra of the Y7W *E. coli* ArsC mutant with various ligands.** Curve 1 is the emission spectrum of 7AW-Y7W ArsC alone. Curve 2 is the emission spectrum of the previous sample with 2  $\mu$ M Grx-1 added. Curve 3 is of the preceding sample with 2 mM arsenate added to the mix. Curve 4 is the preceding sample with 0.5 mM GSH added to the mix. The excitation wavelength was 300 nm, and the 7AW-Y7W ArsC concentration was 2  $\mu$ M. The spectra were all corrected for dilution effects. All samples were prepared in 10 mM Tris, 200 mM NaCl, pH 7.0.

was the case with the A11W mutant, the fluorescence intensity decreased only with the addition of the GSH. The same approach was taken to deduce the cause of the change in fluorescence of the Y7W mutant as the A11W mutant. The results were similar, indicating that the change in fluorescence was due directly to the addition of the GSH and not the Grx-1.

#### 3.10.4 Glutathione Titration of *E. coli* ArsC Mutants

Glutathione titrations were performed on the 7AW incorporated ArsC mutants to see whether there was a direct interaction of the GSH with the mutants. A 2  $\mu$ M sample of 7AW-Y7W ArsC was titrated with GSH ranging in concentration from 5  $\mu$ M (2.5 x the relative amount of ArsC) to 40 mM (20 000 x the relative amount of ArsC). The fluorescence emission spectra of these titrations are presented in Figure 3-17. The fluorescence intensity of the ArsC mutant did not decrease until the GSH concentration reached 100  $\mu$ M, which is 50 x the relative amount of the ArsC mutant. The fluorescence intensity dropped significantly thereafter, with no apparent saturation of quenching even with a GSH concentration of 40 mM. There is no change in the emission max within the titrations, which remained at 367 nm. The 7AW-A11W ArsC mutant results were similar to the Y7W mutant.

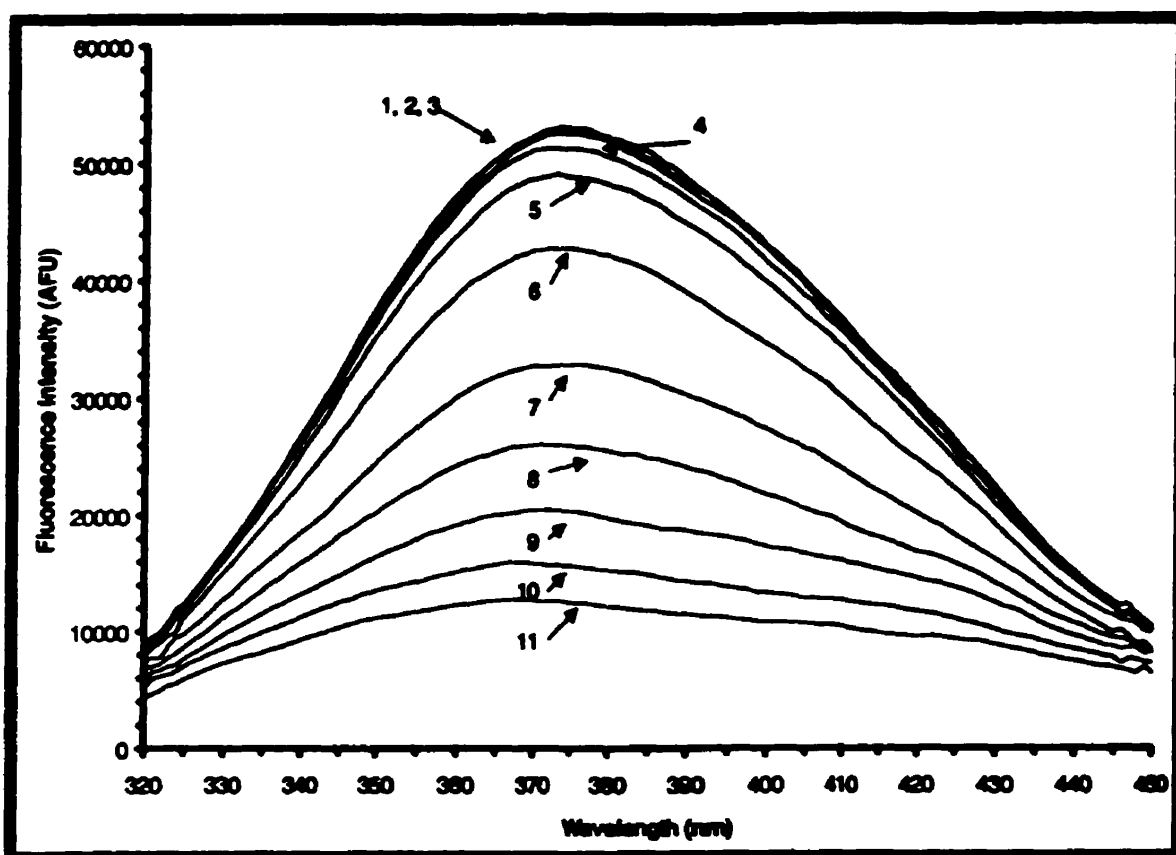


**Figure 3-17: Emission Spectra of the Y7W *E. coli* ArsC mutant with different GSH concentrations.** Curve 1 is the emission spectrum of 7AW-Y7W ArsC alone (2  $\mu$ M). Curve 2 is the emission spectrum of the previous sample with 5  $\mu$ M GSH added. Curve 3 the preceding sample with 50  $\mu$ M GSH added to the mix. Curve 4 is the previous sample with 100  $\mu$ M GSH added to the mix. Curve 5 is the sample with 500  $\mu$ M GSH. Curve 6 has a GSH concentration of 1.0 mM. Curve 7, 8, 9, 10, and 11 have a GSH concentration of 2.0 mM, 5.0 mM, 10 mM, 20 mM, and 40 mM. The excitation wavelength was 300 nm, and the 7AW-Y7W ArsC concentration was 2  $\mu$ M. The spectra were all corrected for dilution effects. All samples were prepared in 10 mM Tris, 200 mM NaCl, pH 7.0.

## **Discussion**

### **4.1 Overexpression and Purification of Proteins**

A typical 2 L culture of the JM109 strain of *E. coli* carrying the ArsC gene grown in 2 x YT medium yielded between 30 - 40 mg of pure ArsC. Overexpression of ArsC was considered successful after visualization of the dense band at 16 000 Daltons in the second lane of Figure 3-3. The purity of the ArsC was considered to be greater than 95 % by visualizing the single band sized at 16 000 Daltons in lane 4 of Figure 3-3.

A typical 2 L culture of the N4830 strain of *E. coli* carrying the pAHOB1 plasmid encoding for Grx-1 yielded between 40 - 50 mg of pure Grx-1. Overexpression of the protein was considered successful after visualization of the dense band at 10 000 Daltons in the second lane of Figure 3-6. The purity of Grx-1 was considered to be greater than 95 % by visualizing the single band of molecular weight 10 kDa in the fourth lane of Figure 3-6.

The A11W and Y7W mutants grown in 2 L of M9 minimal medium supplemented with 7-azatryptophan typically yielded approximately 20 - 30 mg of protein. The lower yields compared to the wild type protein can be attributed to the nutrient-deficient M9 minimal media. The mutated pArsC plasmid was transformed into the W3110A33 strain of *E. coli*, which is incapable of synthesizing its own Trp. The M9 minimal medium is initially supplemented with 4 mg of L-Trp to allow the bacteria to grow prior to overexpression of the desired protein. The bacteria cannot be grown in 7-azatryptophan because not all proteins with the analog incorporated are active. The growth of the bacteria may be impeded if analogues are used initially. Once the bacteria are allowed to grow and have almost exhausted the supply of L-Trp, the addition of 7AW ensures that

there is good incorporation of the analog into the protein being overexpressed. The purity of the A11W and Y7W mutants is displayed in Figure 3-12. The single bands of size 16 kDa in lanes 4 and 7 correspond to the A11W and Y7W mutants of ArsC, respectively.

The purification steps of all of the proteins were completed as quickly as possible, typically taking between 4-5 days. This was done to ensure that as little protein as possible was lost as a result of enzymatic degradation. Enzymatic degradation is evident with the appearance of bands slightly smaller than 16 kDa in a sample of ArsC, indicating that the protein is being nicked into smaller fragments. The proteins collected were of adequate purity for use in fluorescence studies.

#### 4.2 SDS-PAGE of Protein Samples

Gel electrophoresis on a 15% polyacrylamide gel provided a rapid and efficient method to obtain an estimate of the molecular weights and to verify the purity of the fractions isolated from each column during the purification steps. The presence of a single dense band after the elution from the Sephadex G-50 column (Figures 3-3, 3-6, and 3-12) is indicative of a pure, isolated protein sample. The band corresponding to a molecular weight of 16 000 Daltons in Figures 3-3 and 3-12 is confirmation of its being wild type and mutant ArsC, respectively. The molecular weight of wild type ArsC determined by its primary sequence is 15 811 Daltons. The A11W mutant has a molecular weight of 15 926 Daltons (15 928 for the 7AW incorporated mutant) as determined by its primary sequence. The Y7W mutant has a molecular weight of 15 834 Daltons (15 835 for the 7AW incorporated mutant) as determined by its primary

sequence. These values all concur with the molecular weight as determined by 15% SDS-PAGE.

The size of glutaredoxin-1 was estimated to be approximately 10 000 Daltons by 15% SDS-PAGE. The molecular weight of Grx-1 as determined by its primary sequence is 9685 Da. The single dense band in lane 4 of Figure 3-6 is confirmation of the identity and purity of the glutaredoxin-1.

#### 4.3 Amino Acid Analysis of *E. coli* ArsC

Amino acid analysis is a technique used to confirm the identity and also to determine accurately the concentration of a protein. Acid hydrolysis followed by PITC-derivatization and subsequent separation and detection using the Pico-Tag™ system allows for the determination of 17 of the 20 amino acids (Bidlingmeyer *et al.*, 1984). Figure 3-7 is a chromatogram of a hydrolyzed and derivatized ArsC sample. The hydrolyzed and derivatized amino acids elute in order from the smallest and most polar to the largest and least polar. This is because a linear gradient from the initial polar eluent (0.14 M acetate) to a less polar 60% ACN (v/v) eluent is used. The area under each peak was integrated and the molar ratios of each amino acid were quantified using the response factors of derivatized amino acid standards. A comparison of the experimentally determined and expected molar ratios of the detected amino acids is presented in Table 3-1. The correlation is good in most cases. A notable exception is the determined ratios of Asx and Glx. In these cases, the errors are due to the difficulty in resolving these derivatized amino acids. The Asx and Glx differ only by a methylene group, and so resolution of these amino acids can be difficult. This is the most common cause of errors

in the determination of molar ratios. Good solvent preparation and column maintenance help to curb this problem.

The results confirmed the identity of the purified sample as being ArsC. The ratios of almost all of the amino acids were very close to the expected molar ratios (Table 3-1). The concentration of a stock solution of the protein used for circular dichroism experiments was also determined. This was accomplished using the determined molar ratios of alanine and phenylalanine because of their stability to acid hydrolysis. The concentration of ArsC to be used for CD experiments was determined to be 6  $\mu$ M.

#### 4.4 Secondary Structural Studies of *E. coli* ArsC

##### 4.4.1 Prediction of Secondary Structure

A summary of the predicted secondary structures of ArsC using various prediction methods is presented in Table 3-2. The use of prediction algorithms is, as previously mentioned, at least 50 % accurate in most general cases (Voet and Voet, 1990). The predictions are made even more difficult by the fact that the delineation of secondary structures of proteins whose three-dimensional structure is known varies between publications and is most often biased (Fasman, 1989). The algorithms use various techniques and properties such as sequence alignment, hydrophobicity, minimum energy calculations, and physiochemical properties of amino acids to predict secondary structural elements. These algorithms cannot take into account the complex interactions encountered by an intact, three-dimensional, active protein with its environment.

The Chou-Fasman algorithm predicts the structure based on the propensities of amino acids being included in a specific structure. Groups of amino acids with similar



propensities are clustered together and extended, until a residue is encountered that is not disposed to occur in that type of structure (Fasman, 1989). This process is repeated throughout the entire sequence, until the entire polypeptide chain is mapped.

The nnPredict method uses computational neural networks to predict the relation between protein sequence and secondary structure (Kneller *et al.*, 1990). The main advantage of this method is that it is a learning algorithm. The biggest disadvantage is the limited data from which the algorithm can reference and use to predict structures.

The Gibrat method (Gibrat *et al.*, 1987) takes into account the influence of local sequences upon the conformation of a given residue. In this way it is similar to the Chou-Fasman scheme. It differs in that the Gibrat method concentrates on relating residue pairs in lieu of clusters of amino acids.

The Levin method (Levin *et al.*, 1986) is also similar to the Chou-Fasman scheme in that it relates short stretches of amino acids. This method relates stretches of 7 amino acids with homologous sequences of known structures.

The DPM method (Deleage and Roux, 1987) uses a double prediction method consisting of the Chou-Fasman method combined with a prediction of the class of the proteins from their amino acid composition. This has the advantage of combining an already existing method with a novel method.

The Self-Optimized Prediction Method from Alignments (SOPMA) uses multiple alignments of segments with proteins in a database containing 126 chains of dissimilar proteins. The consensus method is a combination of the SOPMA and neural network methods.

The goal of these algorithms is, therefore, to give a general guide into elucidating the actual secondary structure of the protein. This is especially true of ArsC, which does not exhibit any similarity to any known reductases and, hence, cannot be categorized structurally using homology. The best approach would be to use multiple algorithms and deduce a consensus prediction to be used as a guide. All of these algorithms are limited by a finite database of known protein structures. The databases used for each algorithm are modified periodically, contributing further to the variances between determined values. Using this criteria, the prediction of new protein structures using algorithms should increase with the expansion of known protein structures.

#### 4.4.2 Circular Dichroism Studies of *E. coli* ArsC

Circular dichroism is a useful technique for the experimental determination of the secondary structure of a protein. The secondary structural elements of ArsC were estimated using CD spectroscopy in the region from 240 – 190 nm. A spectrum of the reference protein bovine RNase A was also obtained under similar conditions. X-ray data of RNase A (Yang *et al.*, 1986) indicated that the protein contained approximately 24%  $\alpha$ -helix, 33%  $\beta$ -sheet, 14%  $\beta$ -turns, and 29% random coil. NMR data on RNase A (Rico *et al.*, 1991) indicate that the protein contained 21%  $\alpha$ -helix, 33%  $\beta$ -sheet, 12%  $\beta$ -turns, and 34% random coil. The discrepancies between the NMR and X-ray data of bovine RNase A is demonstrative of the largest problem involving protein structure determinations. There is often a lack of agreement between the two methods and, so, the debate on exact structural designations is on going.

Calculations made on the CD spectrum of RNase A indicated that the protein contained approximately 21%  $\alpha$ -helix, 28%  $\beta$ -sheet, 21%  $\beta$ -turns, and 31% random coil using the Hennessey-Johnson database (Hennessey and Johnson, 1981). The CD data is relatively accurate in that it is close to the NMR and X-Ray values for  $\alpha$ -helical,  $\beta$ -sheet, and random coil content, but slightly off in determining the relative amount of turns. The comparison between CD, NMR, and X-ray data for RNase A is favourable, as it validates the relative accuracy of CD in determining secondary structural content.

The calculations made on the ArsC spectrum using the SELCON program (Sreerama and Woody, 1993) indicated approximately 50%  $\alpha$ -helix, 10%  $\beta$ -sheet, 16%  $\beta$ -turns, and 24% random coil. The secondary structure of ArsC did not change significantly with the addition of substrate or product (Table 3-3). The SELCON method of estimating secondary structure is most accurate in estimating the  $\alpha$ -helical content of proteins (Greenfield, 1996). This method is, therefore, a good preliminary estimate for the secondary structure of arsC because of the high  $\alpha$ -helical content of ArsC.

The experimentally determined secondary structure of ArsC compares favourably with the SOPMA and Gibrat methods, and less favourably with the Chou-Fasman, nnPredict, Levin, DPM, and Consensus methods. This is surprising considering that the consensus method is a combination of the SOPMA and neural network methods. On the surface one would think that combining 2 methods of analysis would increase accuracy. The opposite is observed. It seems that the simpler the method the better the estimate. Complex algorithms such as nnPredict do not seem to have any advantages over simpler methods such as the Chou-Fasman method.

#### 4.5 Thermal Denaturation of *E. coli* ArsC

Thermal denaturation studies of ArsC indicated that the melting temperature of ArsC (as monitored by the change in ellipticity at 222 nm using CD spectroscopy) was approximately 46 °C. The melting temperature did not change significantly upon the addition of either arsenate or arsenite (Table 3-4). This is consistent with the data obtained for the secondary structure content of the protein which did not change significantly upon the addition of either arsenate or arsenite.

#### 4.6 Isolation and Site-Directed Mutagenesis of R773 Plasmid Containing the *ArsC* Gene

Isolation of the R773 plasmid was performed using the Pharmacia Flexi-Prep™ Kit. Two 1.5 mL cultures of the JM109 strain of *E. coli* carrying the R773 plasmid grown in 2 x YT media yielded between 15 – 30 ng of the plasmid.

The site-directed mutagenesis of the Ala-11 and Tyr-7 residues was performed using the Stratagene Quik-Change™ site-directed mutagenesis kit. With this kit, the minimal amount of parental plasmid used combined with the low number of PCR cycles helps to ensure that most of the DNA present after thermo-cycling is the mutated plasmid. The *DpnI* restriction enzyme is added to clip only methylated DNA. This ensures that only the parental, non-mutated plasmid DNA is destroyed. The mutated DNA is then transformed into the XL-2 Blue cells which repair the open-ended DNA containing the desired mutation. The transformed XL-2 cells were then plated onto LB-agar plated containing 100 µg/mL ampicillin. A single colony is used to inoculate 50 mL of LB

medium and the mutated plasmid is isolated using the Pharmacia kit. The 2 separate mutants generated, A11W and Y7W, are then ready to be transformed into the Trp auxotroph.

#### **4.7 Transformation of Trp Auxotroph with A11W and Y7W Mutants of ArsC**

The isolated A11W and Y7W mutants of the R773 plasmid were transformed separately into competent W3110A33 Trp auxotroph strain of *E. coli*. Successful transformation resulted in the growth of the transformed cells on LB-agar plates containing 100 µg/mL ampicillin. The resulting plates contained between 10 – 20 individual colonies containing the desired plasmid.

#### **4.8 Isolation of the A11W and Y7W Mutants**

The transformation of the W3110A33 Trp auxotroph was confirmed to be successful, after gel electrophoresis was performed on a sample of an induced culture of each of the mutants. The dense band appearing at 16 kDa is confirmation of successful transformation (Figure 3-12). Purification of the overexpressed ArsC mutants using a Q-Sepharose ion-exchange column and Sephadex G-50 superfine gel filtration results in pure A11W and Y7W mutants of ArsC.

#### **4.9 Fluorescence Studies of Tryptophan Containing *E. coli* ArsC**

The successful site-directed mutagenesis of ArsC was confirmed when a sample of each of the two mutants fluoresced, whereas the wild type did not, when excited at 300 nm (Figure 3-13). The emission maximum of both mutants was 366 nm compared to 412

nm for the free 7-azatryptophan, indicating that the Trp mutants were both similarly buried. The greater fluorescence intensity of the Y7W mutant compared to that of the A11W coupled with the similar emission maximum indicate that there is quenching of the A11W mutant. This is probably due to the proximity of the A11W to the active Cys-12 site, since cysteine is a known quencher of fluorescence (Lakowicz, 1986).

The fluorescence properties of either of the two mutants are not affected by the addition of 2  $\mu$ M Grx-1 (Figures 3-14, 3-15, and 3-16). The indole group of 7-azatryptophan is more sensitive to quenching because of the extra nitrogen atom present. This nitrogen is an extra hydrogen-bond former, hence the greater quenching potential for this analog. The relative intensities of both mutants are decreased upon the addition of GSH, either with or without the presence of Grx-1 and arsenate. This is probably due to the direct interaction of the GSH with the ArsC mutants. The GSH may form a mixed disulfide with the active Cys-12 of ArsC. The results conflict slightly with previous studies (Liu and Rosen, 1997). These results indicated that there was an increase in the fluorescence intensities of both mutants upon the addition of the substrate (arsenate). These studies also indicated that GSH alone did not affect fluorescence. The discrepancies are probably due to the more sensitive nature of 7-azatryptophan. This study does, however, provide supporting evidence for the direct interaction of the 7AW-A11W and 7AW-Y7W mutants with GSH.

#### 4.10 Glutathione Titrations of *E. coli* ArsC

Glutathione titrations of ArsC were performed to confirm a direct interaction between ArsC and GSH. As can be seen in Figure 3-17, the fluorescence intensity begins to

decrease significantly only when the GSH concentration reaches 100  $\mu$ M, which is 50 x the concentration of ArsC. Furthermore, the intensity continues to decrease with the addition of more GSH. This indicates that the interaction between GSH and ArsC is a fluorescent artifact, where the GSH is quenching the intrinsic fluorescence of the protein. It is already known that sulfhydryls are a potent quencher of fluorescence (Lakowicz, 1986), and the increased sensitivity of 7AW relative to L-Trp exaggerates this phenomenon. The final curve in Figure 3-17 demonstrates how the fluorescence intensity was continually decreasing with the GSH concentration at 40 mM, which is 20 000 times the concentration of ArsC. If the interaction between the protein and GSH were some kind of ligand interaction such as disulfide bond formation between ArsC and GSH, then the change in fluorescence properties would exhibit saturation. This is not seen, and the interaction is merely the quenching effect of GSH.

#### 4.11 Conclusions

The reaction scheme for arsenate reduction is believed to have at least two steps: the ArsC reduces the arsenate to arsenite, becoming oxidized itself; and secondly, the Grx-1 reduces the arsenate, thereby regenerating the enzyme. The Grx-1 is proposed to be reduced by glutathione. Recent studies (Liu and Rosen, 1997) indicate that the glutathione may act directly with the ArsC in addition to regenerating Grx-1. These results concur with the fluorescence studies on the 7AW-incorporated ArsC mutants, which demonstrate a direct interaction of GSH with the 7AW mutants (Figures 3-15 and 3-16). The 7AW mutants do not, however, provide evidence for the formation of an ArsC-arsenate or ArsC-Grx-1 complex. The results also do not provide evidence for the

formation of an ArsC-GSH complex. Further investigation is required to elucidate the exact mechanism of arsenate reduction with ArsC. The proposed mechanism of arsenate reduction by ArsC is presented in Figure 4-1. It proposes that an initial complex is formed between ArsC and the arsenate (Liu and Rosen, 1997). This complex would then interact with GSH, with the transfer of electrons to reduce  $As^{5+}$  to  $As^{3+}$ . The resulting arsenite would then dissociate from the complex, with its subsequent extrusion by ArsA and ArsB. The ArsC-GSH would then be reduced by Grx-1, regenerating reduced ArsC. The glutathione-glutaredoxin complex would then be reduced by additional GSH, indicating dual role for GSH. The result is the regeneration of Grx-1 and GSSG, which itself can be reduced by glutathione reductase and NADPH. This mechanism model provides a testable scheme for the interactions between ArsC, Grx-1, GSH, and arsenate.

#### 4.12 Future Work

The goal of using the analog incorporated mutants is to allow for the use of fluorescence studies to probe into the interactions of two proteins in cases where both of the proteins contain Trp. In this case, the Grx-1 contains a Trp residue that is solvent exposed and, hence, contributes to the fluorescence signal without aiding in the interaction studies. Activity assays of the 7AW-A11W and 7AW-Y7W mutants must be performed to determine whether the incorporation of the analog affects activity. If inactive, other analogues (e.g. 5-fluorotryptophan, 5-hydroxytryptophan) can be incorporated into the Trp mutants which may not affect the activity of the protein.

Recent focus has been on using another glutaredoxin, glutaredoxin-3, which does not contain any Trp residues (Nordstrand *et al.*, 1999). This would eliminate the need for



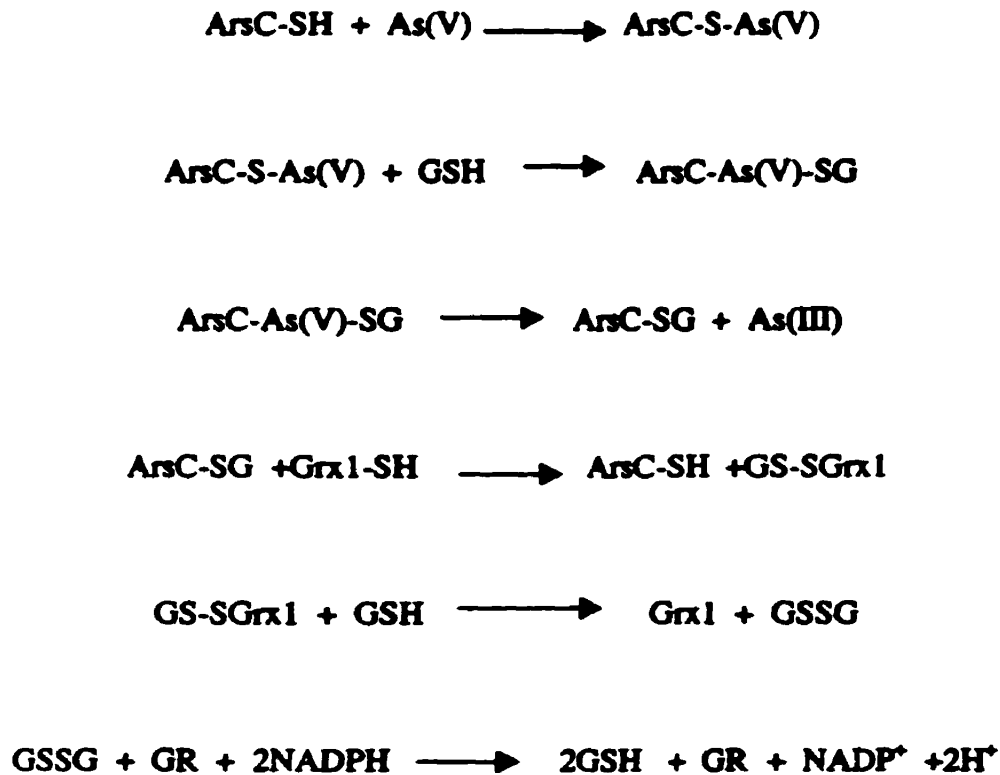


**Figure 4-1: Proposed Mechanism of Arsenate Reduction.** An initial complex is formed between ArsC and the arsenate. This complex would then interact with GSH, with the transfer of electrons to reduce  $\text{As}^{5+}$  to  $\text{As}^{3+}$ . The resulting arsenite would then dissociate from the complex, with its subsequent extrusion by ArsA and ArsB. The ArsC-GSH would then be reduced by Grx-1, regenerating reduced ArsC. The glutathione-glutaredoxin complex would then be reduced by additional GSH, indicating a dual role for GSH. The result is the regeneration of Grx-1 and GSSG, which itself can be reduced by glutathione reductase (GR) and NADPH. This mechanism model provides a testable scheme for the interactions between ArsC, Grx-1, GSH, and arsenate (Liu and Rosen, 1997).

using analog-incorporated mutants which always poses the question of whether or not the protein is active. *E. coli* glutaredoxin-3 displays a 33% sequence homology to *E. coli* glutaredoxin-1 (Aslund *et al.*, 1996). Both glutaredoxins contain the Cys-Pro-Tyr-Cys redox-active motif, indicating similar reaction schemes. Grx-3 interaction studies with ArsC using fluorescence spectroscopy could, therefore, potentially shed more light on the proposed mechanism arsenate reduction. The complexity of ArsC activity and its novel reductase properties make the elucidation of its reaction pathway an important area of investigation for future work.

## References

- Adler, A.J., Greenfield, N.J., Fasman, G.D. (1973) Circular dichroism and optical rotatory dispersion of proteins and polypeptides. *Methods Enzymol.* **27**, 675-735.
- Aslund, F., Ehn, B., Miranda-Visuete, A., Pueyo, C., and Holmgren, A. (1994) Two additional glutaredoxins exist in *Escherichia coli*: glutaredoxin 3 is a hydrogen donor for ribonucleotide reductase in a thioredoxin/glutaredoxin-1 double mutant. *Proc. Natl. Acad. Sci., U. S. A.* **91**, 9613-9617.
- Bidlingmeyer, B.A., Cohen S.A., Tarvin T.L. (1984) Rapid analysis of amino acids using pre-column derivatization. *J. Chromatogr.* **336**, 93-104.
- Bjornberg, O., and Holmgren, A. (1991) Characterization of homogeneous recombinant glutaredoxin from *Escherichia coli*: purification from an inducible lambda-PL expression system and properties of a novel elongated form. *Protein Expression Purif.* **2**, 287-295.
- Chen, C.M., Misra, T., Silver, S., and Rosen, B.P. (1986) Nucleotide sequence of the structural genes for an anion pump. The plasmid-encoded arsenical resistance operon. *J. Biol. Chem.* **261**, 15030-15038.
- Chen, Y. and Rosen, B.P. (1997) Metalloregulatory Properties of the ArsD Repressor. *J. Biol. Chem.* **272**, 14257-14262.

Ching, M.H., Kaur, P., Karkaria, C.E., Steiner, R.F., and Rosen, B.P. (1991) Substrate-induced dimerization of the ArsA protein, the catalytic component of an anion-translocating ATPase. *J. Biol. Chem.* **266**, 2327-2332.

Chou, P.Y., and Fasman, G.D. (1978), Prediction of the secondary structure of proteins from their amino acid sequence. *Adv Enzymol Relat Areas Mol Biol.* **47**, 45-148.

Deleage, G., Roux, B. (1987) An algorithm for protein secondary structure prediction based on class prediction. *Protein Eng.* **1**, 289-294.

Dey, S. Dou., D., and Rosen, B.P. (1994) ATP-dependent arsenite transport in everted membrane vesicles of Escherichia coli. *J. Biol. Chem.* **269**, 25442-25446.

Fasman, G.D. (1989) Prediction of Protein Structure and the Principles of Protein Conformation. Plenum Press, N.Y., pp 281-360.

Geourjon, C., Deleage G. (1995) SOPMA: significant improvements in protein secondary structure prediction by consensus prediction from multiple alignments. *Comput. Appl Biosci.* **11**, 681-684.

Gibrat, J.F., Garnier J., Robson B., (1987) Further developments of protein secondary structure prediction using information theory. New parameters and consideration of residue pairs. *J. Mol. Biol.* **198**, 425-443.

Gladeysheva, T.B., Oden, K.L., and Rosen, B.P. (1994) Properties of the arsenate reductase of plasmid R773. *Biochemistry* 33, 7288-7293.

Greenfield, N.J. (1996) Methods to estimate the conformation of proteins and polypeptides from circular dichroism data. *Anal. Biochem.* 235, 1-10.

Hedges, R.W., and Baumberg, S. (1973) Resistance to arsenic compounds conferred by a plasmid transmissible between strains of *Escherichia coli*. *J. Bacteriol.* 115, 459-460.

Hennessey, J.P., and Johnson, W.C., Jr. (1981) Information content in the circular dichroism of proteins. *Biochemistry* 20, 1085-1094.

Hogue, C.W. and Szabo, A.G. (1993) Characterization of aminoacyl-adenylates in *B. subtilis* tryptophanyl-tRNA synthetase, by the fluorescence of tryptophan analogs 5-hydroxytryptophan and 7-azatryptophan. *Biophys Chem.* 48, 159-169.

Holmgren, A. (1989) Thioredoxin and glutaredoxin systems. *J. Biol. Chem.* 264, 13963-13966.

Hudson, B.S., Harris, D.L., Ludescher, R.D., Ruggiero, A., Cooney-Freed, A., and Vavalier, S. (1986) in Applications of Fluorescence in the Biomedical Sciences, New York: A.R. Liss, pp 159-202.

Ji., G., Garber, E.A.E., Armes, L.G., Chen, C.-M., Fuchs, J.A., and Silver, S. (1994) Arsenate reductase of *Staphylococcus aureus* plasmid pI258. *Biochemistry* **33**, 7294-7297.

Ji, G., and Silver, S. (1992) Energy-dependent arsenate efflux: the mechanism of plasmid-mediated resistance. *J. Bacteriol.* **174**, 3684-3694.

Kabsch, W., and Sander, C. (1983) Dictionary of protein secondary structure: pattern recognition of hydrogen-bonded and geometrical features. *Biopolymers* **22**, 2577-2637.

Kahn, T.W., Sturtevant, J.M., Engelman, D.M. (1992) Thermodynamic measurements of the contributions of helix-connecting loops and of retinal to the stability of bacteriorhodopsin. *Biochemistry* **31**, 8829-8839.

Kneller, D.G., Cohen F.E., Langridge R. (1990) Improvements in protein secondary structure prediction by an enhanced neural network. *J. Mol. Biol.* **214**, 171-182.

Knowles, F.C. and Benson, A.A. (1983) The enzyme inhibitory form of inorganic arsenic. *Trends Biochem. Sci.* **8**, 178-180.

Laemmli, U.K. (1970) Cleavage of structural proteins during the assembly of the head of bacteriophage T4. *Nature* **227**, 680-685.

Lakowicz, J.R. (1986) Principles of Fluorescence Spectroscopy. Plenum Press, N.Y., pp. 257-381.

Levin, J.M., Robson, B., Garnier, J. (1986) An algorithm for secondary structure determination in proteins based on sequence similarity. *FEBS Lett.* **205**, 303-308.

Li, J., Liu, S., and Rosen, B.P. (1996) Interaction of ATP binding sites in the ArsA ATPase, the catalytic subunit of the Ars pump. *J. Biol. Chem.* **271**, 25247-25252.

Liu J., and Rosen B.P. (1997) Ligand Interactions of ArsC Arsenate Reductase. *J. Biol. Chem.* **272**, 21084-21089.

Lowry, L.H., Rosebrough, N.J., Farr, A.L., and Randall, R.J. (1951) *J. Biol. Chem.* **193**, 265-275.

Micklos, D.A., and Freyer, G.A. (1990) DNA Science: A First Course in Recombinant DNA Technology, Cold Spring Harbour Laboratory Press, NC, pages 366-382.

Miller, J.H. (1972) in Experiments in molecular genetics, Cold Spring Harbor Laboratory, Cold Spring Harbour, NY. (466 pages).

Mobley, H.L.T., and Rosen, B.P. (1982) Energetics of plasmid-mediated arsenate resistance in *Escherichia coli*. *Proc. Natl. Acad. Sci.* **79**, 6119-6122.

Nordstrand, K., Aslund, F., Holmgren, A., Otting, G., and Berndt, K.D. (1999) NMR structure of *Escherichia coli* glutaredoxin 3-glutathione mixed disulfide complex: implications for the enzymatic mechanism. *J Mol Biol.* **286** (2), 541-542.

Novick, R.P., and Roth, C. (1968) Plasmid-linked resistance to inorganic salts in *Staphylococcus aureus*. *J. Bacteriol.* **95**, 1335-1342.

Rico, M., Santoro, J., Gonzalez, C., Bruix, M., Neira, J.L., Nieto, J.L., and Herranz, J. (1991) 3D structure of bovine pancreatic ribonuclease A in aqueous solution: an approach to tertiary structure determination from a small basis of <sup>1</sup>H NMR NOE correlations. *J. Biomol. NMR* **1**, 283-298.

Rosen, B.P., Weigel, U., Monticello, R. A., & Edwards, B.P.F., (1991) Molecular analysis of an anion pump: purification of the ArsC protein. *Arch. Biochem. Biophys.* **284**, 381-385.

Ross, J.B., Szabo, A.G., Hogue, C.W. (1997) Enhancement of protein spectra with tryptophan analogs: fluorescence spectroscopy of protein-protein and protein-nucleic acid interactions. *Methods Enzymol.* **278**, 151-190.

Rost, B., Sander, C., Schneider, R. (1994) PHD—an automatic mail server for protein secondary structure prediction. *Comput. Appl. Biosci.* **10**, 53-60.



San Francisco, M.J.D., Hope, C.L., Owolabi, J.B., Tisa, L.S., and Rosen, B.P.. (1990) Identification of the metalloregulatory element of the plasmid-encoded arsenical resistance operon. *Nucleic Acids Res.* **18**, 619-624.

Silver, S. (1992) Plasmid-determined metal resistance mechanisms: range and overview. *Plasmid* **27**, 1-3.

Silver, S. and Phung, L.T. (1996) Bacterial Heavy Metal Resistance: New Surprises. *Annu. Rev. Microbiol.* **50**, 753-789.

Sreerama, N., Woody, R.W. (1993) A self-consistent method for the analysis of protein secondary structure from circular dichroism. *Anal. Biochem.* **209**, 32-44.

Sykes, B.D., Weingarten, H.I., and Schlesinger, M.J. (1974) Fluorotyrosine alkaline phosphatase from *Escherichia coli*: preparation, properties, and fluorine-19 nuclear magnetic resonance spectrum. *Proc. Natl. Acad. Sci. U. S. A.* **71**, 469-473.

Taylor, J.W. and Eckstein, F. (1985) The rapid generation of oligonucleotide-directed mutations at high frequency using phosphorothioate-modified DNA. *Nucleic Acid Res.* **13**, 8765-8785.

Tisa, L.S., and Rosen, B.P. (1990) Molecular characterization of an anion pump. The ArsB protein is the membrane anchor for the ArsA protein. *J. Biol. Chem.* **265**, 190-194.

Voet, D. and Voet, J.G. (1990) Biochemistry, John Wiley and Sons, N.Y., pp. 200-205.

Willsky, G.R., and Malamy, M.H. (1981) Effect of arsenate on inorganic phosphate transport in *Escherichia coli*. *J. Bacteriol.* **144**, 366-374.

Wu, J.H., and Rosen, B.P. (1991) The ArsR protein is a trans-acting regulatory protein. *Mol. Microbiol.* **5**, 1331-1336.

Yang, J.T., Wu, C.S.C., Martinez, H.M. (1986) Calculation of protein conformation from circular dichroism. *Methods in Enzymology* **130**, 208-248.

Xu, C. and Rosen, B.P. (1997) Dimerization is Essential for DNA binding and repression by the ArsR metalloregulatory protein of *E. coli*. *J. Biol. Chem.* **272**, 15734-15738.

## **VITA AUCTORIS**

### **DOMENIC PERRI**

<b>BIRTHDATE</b>	<b>May 26, 1970</b>	
<b>EDUCATION</b>	<b>1989 - 1996</b>	<b>Honours B. Sc. Biochemistry University of Windsor, Windsor, Ontario</b>
	<b>1996 - present</b>	<b>M. Sc. Candidate University of Windsor, Windsor, Ontario</b>

### **SCHOLARSHIPS AND AWARDS**

<b>1989</b>	<b>University of Windsor Entrance Scholarship</b>
<b>1989</b>	<b>Canada Scholars Scholarship</b>